UNIVERSITA' DEGLI STUDI DI NAPOLI
"FEDERICO II"

DOTTORATO DI RICERCA IN
BIOLOGIA APPLICATA

XXV CICLO
(2011-2013)

Human DNA replication factors:
new interactions and functional significance

Dottoranda:
Mariarosaria De Falco

Tutor:
Prof. Sergio Esposito

Coordinatore:
Prof. Ezio Ricca

TABLE OF CONTENTS

Chapter 1 1

1.1. INTRODUCTION 3

1.1.1. Eukaryotic cell cycle and its regulation 3

1.1.2. Genome stability 5

1.1.3. Activation of pre-replicative complex 5

1.1.4. Eukaryotic replicative DNA polymerases 6

1.1.5. Mcm10 8

1.2. REFERENCES 13

Chapter 2

The mini-chromosome maintenance (Mcm) complex interacts with DNA polymerase α-primase and stimulates its ability to synthesize RNA primers 15

2.1 INTRODUCTION 19

2.2 RESULTS 25

2.2.1. Mcm forms a complex with the DNA polymerase α-primase or DNA primase 25

2.2.2. Physical interactions between Mcm and primase 27

2.2.3. Influence on the DNA-binding activities of Mcm4/6/7 and primase .. 29

2.2.4. Effect of primase on Mcm helicase and ATPase activities 32

2.2.5. Mcm stimulates RNA primer synthesis by primase 34

2.3 DISCUSSION 39

2.4 MATERIALS AND METHODS 45

2.4.1. Expression and purification of recombinant proteins in insect cells and *E. coli* 45

2.4.2. Reagents 45

2.4.3. Construction of DNA substrates 45

2.4.4. Primer RNA synthesis assays. 46

2.4.5. DNA-binding and helicase assays 47

2.4.6. ATPase assays 47

2.4.7. Immuno-precipitation (IP) analyses 47

2.4.8. Immunoprecipitation experiments on insect cells co-infected with baculoviruses 48

2.4.9. Glycerol gradient fractionation 48

2.5. REFERENCES 51

Chapter 3

The physical interaction of Mcm10 with Cdc45 modulates their DNA binding properties 57

3.1. INTRODUCTION 61

3.2. RESULTS 67

3.2.1. Mcm10 and Cdc45 interact in human cells 67

3.2.3. Physical interaction of Mcm10 domains with Cdc45 70

3.2.4. DNA binding activity of the Mcm10 domains 73

3.2.5. Mcm10 ID cooperates with Cdc45 in binding DNA 77

3.2.6. Mcm10 CTD, but not NTD, cooperates with Cdc45 in binding DNA 78

3.3. DISCUSSION 83

3.4. MATERIALS AND METHODS 91

3.4.1. Production of recombinant proteins 91

3.4.2. Co-immunoprecipitation experiments 92

3.4.3. Surface plasmon resonance measurements 93

3.4.4. DNA substrates 94

3.4.5. DNA band-shift assays 94

3.4.5. Domain structure fitting 94

3.5. REFERENCES..... 99

Chapter 1

Introduction

1.1. INTRODUCTION

1.1.1. EUKARYOTIC CELL CYCLE AND ITS REGULATION

DNA replication is an intricate process requiring the concerted action of many different proteins. The transmission of genetic information from one generation to the next requires that the parental genome is replicated exactly once in each generation.

The copying of the parental DNA duplex is carried out by a multiprotein machine, the replisome, which is assembled in a controlled manner at chromosomal sites, termed replication origins, which contains DNA sequences recognized by replication initiator. It proceeds in three main steps: initiation, elongation and termination.

Eukaryotic genomes are replicated from multiple replication origins distributed along multiple chromosomes. This strategy has an important advantage: the time required to replicate the entire genome is no longer proportional to genome size, but, to a first approximation, is proportional to the inter-origin distance. Thus, large genomes can be replicated in short periods of time. However, in order to achieve precise genome duplication, it is crucial that the activity of these multiple origins is carefully coordinated.

The eukaryotic cell cycle consists of four phases (Fig.1): G1, S (DNA synthesis [Umar A & Kunkel TA (1996), Koepp DM (2010), Atkinson J and McGlynn P (2009)], G2 and M (mitosis). Just before the genome duplication, the cell prepares its genome for DNA replication, this phase is the so-called Gap1 (G1). Similarly, in the second gap phase (G2), the cell oversees that the process of genome duplication has been correctly executed and prepares for mitosis. Failure to accumulate the necessary replication factors in G1 or evidence of a not corrected genome duplication in G2, causes a block of the cell cycle before the onset of S and M phases, respectively. The G1 and G2 phases are also used by the cell to check the quality of the genetic information and to repair DNA damages when present. Checkpoints are also operating during S and M phases, in order to avoid incomplete genome duplication or re-duplication, as well as unbalanced chromosome segregation.

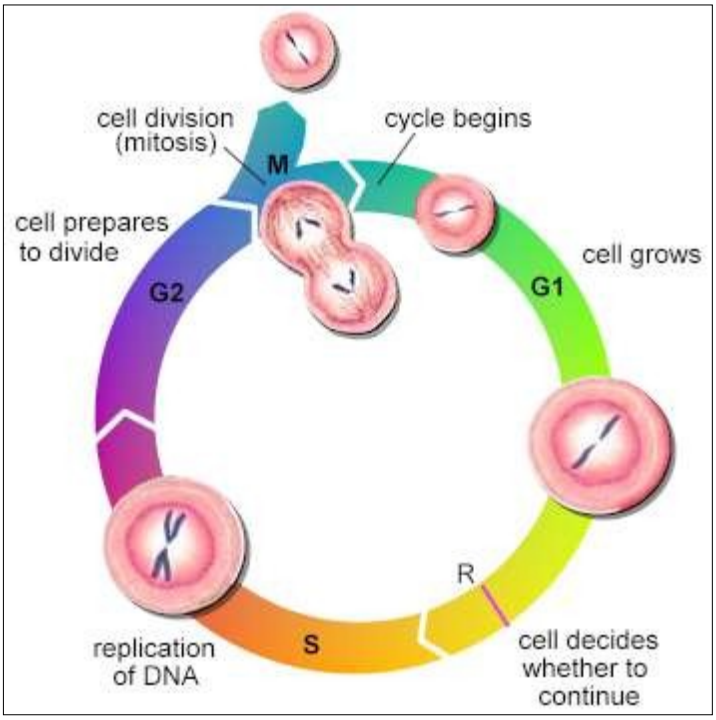

Figure 1. The cell cycle is divided in two main parts: interphase and mitosis. During interphase the cell grows and replicates its chromosomes. Interphase is subdivided into three phases: gap phase 1 (G1), synthesis (S) and gap phase 2 (G2). (Image from "The Encyclopedia of Science").

The chromosome replication cycle in eukaryotes is strictly divided into a period when replication origins acquire replication competence (licensing) but are inactive, and a subsequent period during which origins can be activated but cannot be re-licensed [Bell SP, Dutta A (2002), Diffley JF (2004)]. Replication competence is conferred by Mcm2-7 loading. During this period, Mcm2-7 remain stationary at replication origins and unwound DNA is not yet detected [Geraghty DS (2000)].

The vast majority of the cells in an adult organism, undergo terminal differentiation and lose their ability to proliferate. Other cells exit the normal cell cycle and enter a special stage of quiescence (called G0), whose length is variable. However, these cells maintain their proliferative potential and, under the appropriate external stimuli (for example a rise in the levels of specific proliferative factors), re-entry into the cell cycle is triggered.

If a cell, within this proliferation-competent population, loses its ability to control the genome duplication process, it can acquire a tumorigenic phenotype,

ultimately leading to the development of cancer. Indeed, it is now clear that genome over- or under-replication will cause genome instability, which is the hallmark of cancer.

1.1.2. GENOME STABILITY

The maintenance of genomic stability is critical for the normal growth and development of any living organism and perturbations of this highly regulated equilibrium, leading to genomic instability, has been linked to the development of cancers and other disease states [Bogliolo M. et al. (2002), Umar A & Kunkel TA (1996)]. Genomic stability can be defined as the ability of a cell to pass its genetic information to the progeny, without either loss or duplication of genome sequences. Two events are crucial to this process: the faithful duplication of the cellular genome and the correct segregation of the duplicated chromosomes into the daughter cells. To maintain genome integrity, cells have developed a highly orchestrated process to ensure accurate inheritance of genetic information to one generation to the next and a single duplication of the entire genome during each round of cell division.

Thus, understanding at the molecular level those pathways orchestrating the exact execution of DNA replication is of essence for our comprehension of the molecular basis of cancer, as well as for developing novel therapeutic approaches.

Mammalian genomes range from ~10^7 up to > 10^{11} bps, but they are not a long continuous thread of DNA. In humans, the genome is divided into 46 chromosomes per diploid cell, each chromosome containing thousands of replication origines. Regardless of the size of the genome, all of the chromosomal DNA sequence must be precisely replicated once and only once in each cell cycle.

In eukaryotic systems, replication initiation is a cell cycle-regulated process characterized by a multi-step sequential loading of many proteins onto the DNA.

1.1.3. ACTIVATION OF PRE-REPLICATIVE COMPLEX

One key component of the DNA replication machinery is the pre-replication complex (pre-RC). The process of pre-RC assembly on origins is also known as replication licensing, which is the key step in initiating DNA replication. Proper

control of replication licensing is essential for re-replication prevention and contributes to the maintenance of genome integrity. Therefore, it is not surprising that dys-regulation of DNA replication licensing factors is associated with many human diseases, including cancers.

At the heart of the pre-RC lies the origin recognition complex (ORC) which is composed by six different subunits (Orc1 to Orc6) [Bell SP & Stillman B (1992)]. In higher eukaryotes, during late M/early G1, ORC recognizes and binds the origin and remains bound to chromatin at all the subsequent stages. It then promotes the sequential recruitment of two additional proteins: the cell division cycle 6 (Cdc6), and the DNA replication factor Cdt1. These proteins cooperatively act to recruit a complex of six proteins called *m*ini-chromosome *m*aintenance (MCM) 2-7 to the origin. Together, ORC, Cdc6, Cdt1 and MCM2–7 constitute the pre-replication complex (pre-RC) [for review, Bell SP & Dutta A (2002)] that remains chromatin-bound until late G1 phase.

At this point a cascade of several phosphorylation events occurs that enable the subsequent loading of two helicase co-factors, Cdc45 and GINS complex to form the pre-IC. Mcm together with Cdc45 and GINS forms the CMG complex, the active replicative helicase. Now the complex is activated and this activation results in the unwinding of replication origins, the recruitment of DNA pols and accessory factors and the assembly of the replisome for the DNA synthesis

The point where the DNA is separated into single strands, and where new DNA will be synthesized, is known as the replication fork (Fig.2)

1.1.4. EUKARYOTIC REPLICATIVE DNA POLYMERASES

DNA replication is accomplished by a suite of three polymerases: the primase DNA polymerase α (Pol α), and the main replicative polymerases DNA polymerase δ (Pol δ) and DNA polymerase ε (Pol ε), which catalyze DNA synthesis on opposite strands [Nick McElhinny et al., 2008]

The eukaryotic DNA polymerases are well-conserved in terms of overall architecture and sequence, especially within the catalytic domain

Pol α , Pol δ , and Pol ε are members of Family B Polymerases and are the main polymerases involved with nuclear DNA replication.

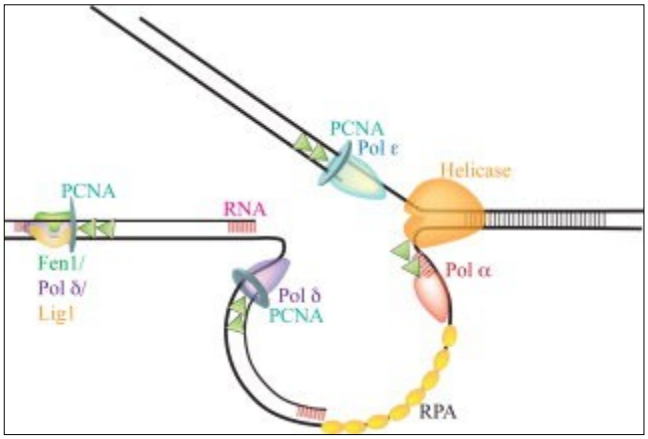

Figure 2 Model of the eukaryotic replication fork. The current model, showing Okazaki fragments at three stages of formation. Next to the MCM helicase, the primase Pol α synthesizes an RNA primer (pink box with lines) and a small amount of DNA, beginning lagging strand synthesis. Replication protein A (RPA) coats the single-stranded DNA between the Pol α-catalyzed primers. The next primer has been extended by the lagging strand replisome, represented by Pol δ and PCNA. The third Okazaki fragment has been completely extended, and Okazaki fragment maturation, directed by Pol δ, Fen1, and Lig1, is underway. The leading strand is shown as being copied by Pol ε and PCNA, although Pol δ may be responsible for some leading strand synthesis as well. Several important cofactors are not shown for simplicity. Figure inspired by and adapted with permission from Burgers, J Biol Chem,(2009), 284, 4041-4045,

In all eukaryotic organisms, Pol α is a heterotetrameric enzyme. Three separate domains were identified in the catalytic p180 subunit. The heterotetrameric pol α is unique among eukaryotic pols, since two of the three small subunits have DNA primase activity. The heterodimeric DNA primase is associated with the catalytic 180-kDa subunit and the B subunit [Arezi B & Kuchta RD. (2000)]. Like the corresponding polypeptides in pol δ and pol ε heteromultimers, the B subunit of Pol α has no detectable enzymatic activity, but is essential in yeast and appears to have a role in maintaining a functional heterotetrameric complex. In addition, the finding that it is phosphorylated in a cell-cycle-dependent manner suggests regulatory functions [Mizuno T, et al. (1999)].

The presence of the primase activity confers to Pol α the role of initiation of DNA polymerization. Once primase has created the RNA primer, Pol α starts replication elongating the primer with ~20 nucleotides. Due to their high processivity, Pol ε and Pol δ take over the leading and lagging strand synthesis from Pol α

respectively [Nick McElhinny SA et al (2008)]

DNA polymerase blockage leads to replication arrest and can gives rise to genome instability.

1.1.5. MCM10

Recent studies have shown that dys-regulation of the assembly of the pre-RC components, as well as of their upstream regulators, is observed in many types of cancer cells, such as breast, brain, prostate, oral, colorectal, ovarian, kidney, bladder, and hematological cancers [for reviews, Hook SS, et al. (2007), Williams GH & Stoeber K (2007)].

In addition, the combined action of two S phase promoting kinases, the cyclin-dependent (CDK) and Cdc7-Dbf4 (DDK) kinases is required to activate replication [Sclafani RA & Holzen TM (2007)]. Protein phosphorylation is a fundamental mechanism to ensure proper progression of the cell cycle, including replication licensing. Almost every component of the pre-RC complex is subjected to phosphorylation. In general, phosphorylation of licensing proteins exerts its regulatory function by targeting the proteins for ubiquitylation and subsequent proteolysis, by mediating interaction with specific inhibitors, or by directing translocation of the proteins to cytoplasm to prevent pre-RC formation. However, much has to be learned about the phosphorylation of pre-RC components and how this event modifies their functional properties. In fact, in recent years, in addition to the above-mentioned components, additional factors have been identified as essential for the assembly of the DNA unwinding complex, including Dpb11/Cut5, Sld2, Sld3, and MCM10. The combined action of these proteins is critical for the loading of Cdc45 and GINS onto replication origins and the assembly of the DNA unwinding complex but how these proteins act remains unclear.

The essential requirement of MCM10 in DNA replication initiation and elongation was demonstrated to be conserved in eukaryotes. Mutations in MCM10 cause a decrease in initiation of replication, slow progression of DNA synthesis and stalling replication forks during elongation [Homesley L et al. (2000)]. Since MCM10 is essential for replication initiation and elongation, its

activity is regulated in a cell-cycle manner to ensure a single round of replication. Human MCM10 protein is known to decrease in the early G1 phase [Homesley L et al. (2000)]. In eukaryotes MCM10 is an ubiquitous protein; it contains a CCCH-type Zn-finger that is necessary for its self-assembly into homo-complexes which are essential for growth in budding yeast.

Although the step at which MCM10 is recruited to the replication origin remains debatable and may vary among species, it has been proven that MCM10 is essential for replication initiation and elongation steps (see Fig.3). Therefore, it is expected that cells must tightly regulate the activity of MCM10. This protein, after replication initiation, seems to travel along with the replication fork and undergoes inhibitory phosphorylation at the end of the S phase, where its activity needs to be curtailed, leading to its dissociation from chromatin at G_2 phase and eventually degradation in mitosis [Izumi M et al. (2000), Izumi M et al. (2001), Izumi M et al. (2004)].

A detailed biochemical analysis of the human MCM10 is still missing. Surely, new findings on the role of MCM10 in initiation and elongation phases of DNA replication can greatly encourage development of novel anticancer drugs and may establish a new mode for chemotherapy. Understanding the details of MCM10 biological function and its regulation during cell cycle is the principal aim of this work.

Moreover delineating the steps involved in initiation and replication of DNA characterizing the molecular events involved in the process will yield important insight into the molecular mechanisms by which cell cycle progression is controlled.

Proper regulation of DNA replication is crucial to the fate of cells. DNA replication initiation represents a point of convergence of numerous signaling pathways involved in cell cycle progression. Understanding cellular mechanisms that regulate DNA replication will greatly benefit the chemotherapies of human.

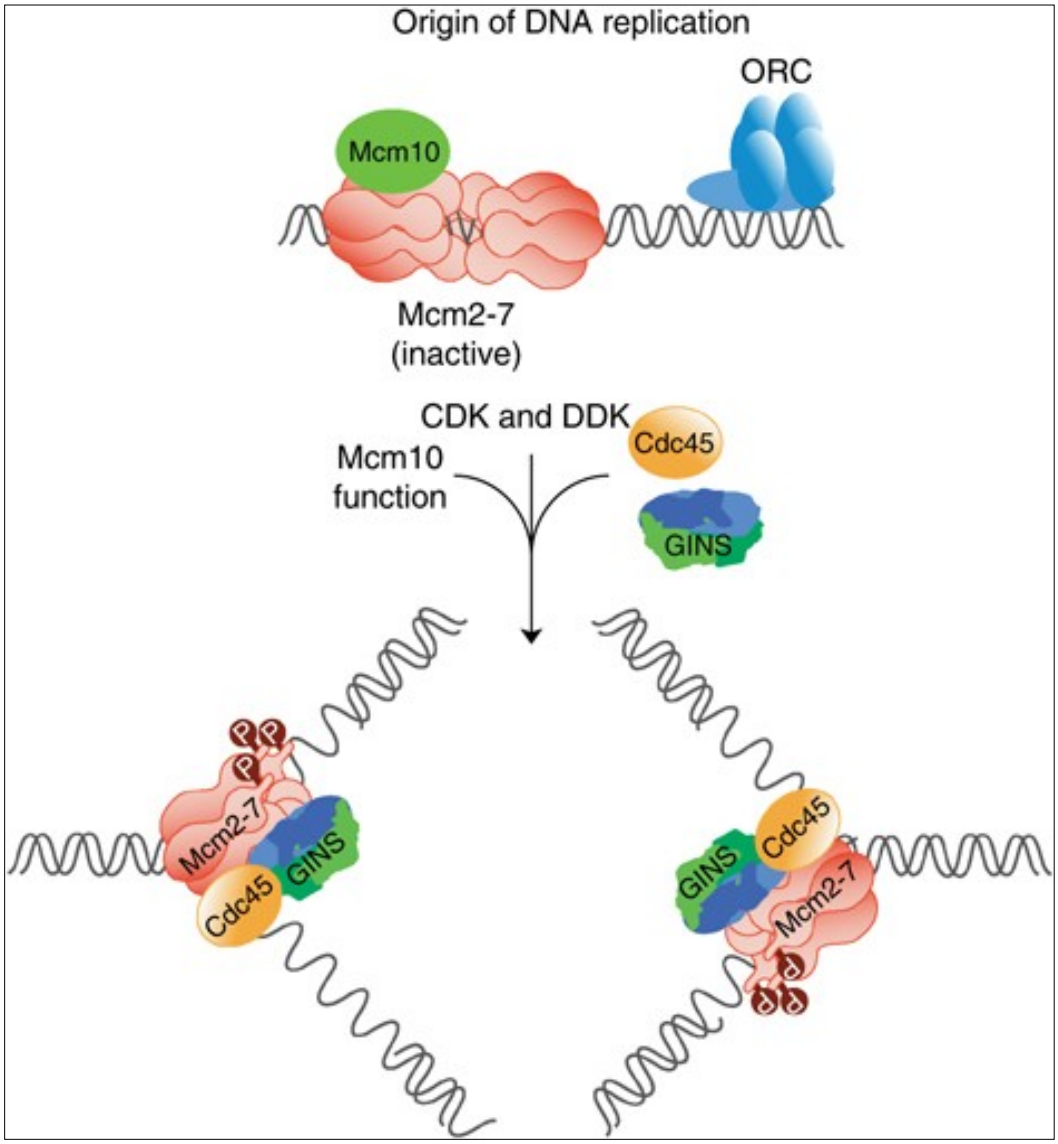

Figure 3 Model for the activation of Cdc45–MCM–GINS helicase during the initiation of chromosome replication. Mcm10 associates with the loaded Mcm2-7 complex at origins of DNA replication. As cells enter S-phase, activation of cyclin-dependent kinase (CDK) and Cdc7 kinase mediates the recruitment of GINS and Cdc45, respectively [Heller et al., (2011)]. Mcm10 is dispensable for the recruitment of GINS and Cdc45 to the loaded Mcm2-7 complex in budding yeast, and does not appear to be a stable subunit of the active Cdc45–MCM–GINS helicase at replication forks. Instead, we propose that Mcm10 is required for a novel step of the initiation reaction that is required for activation of the loaded Mcm2-7 complex at replication origins *in vivo*—see text for further details. For the sake of simplicity, other replisome components have been omitted, and the presumed association of Mcm10 with replication forks is not shown.

Figure 6 from Frederick van Deursen et al.
The EMBO Journal on line publication 20 march 2012

References

1.2. REFERENCES

- Arezi B & Kuchta RD. (2000), Eukaryotic DNA primase, *Trends Biochem. Sci.***25**:572–76
- Atkinson J & McGlynn P (2009) Replication fork reversal and the maintenance of genome stability *Nucleic Acids Res.* **37**:3475–3492.
- Bell SP & Dutta A (2002), DNA replication in eukaryotic cells. *Annu Rev Biochem,* **71**:333-374
- Bell SP & Stillman B (1992) ATP-dependent recognition of eukaryotic origins of DNA replication by a multiprotein complex, *Nature* **357**:128-34
- Bogliolo M, Cabre O, Callen E, Castillo V, Creus A, Marcos R and Surralles J, (2002), The Fanconi anaemia genome stability and tumour suppressor network *Mutagenesis* **17**:529–538
- Diffley JF: (2004) Regulation of early events in chromosome replication. *Curr Biol*, **14:**R778-786
- Geraghty DS, Ding M, Heintz NH, Pederson DS (2000), Premature structural changes at replication origins in a yeast minichromosome maintenance (MCM) mutant. J Biol Chem, **275**:18011-18021
- Heller RC, Kang S, Lam WM, Chen S, Chan CS, Bell SP (2011), Eukaryotic origin-dependent DNA replication in vitro reveals sequential action of DDK and S-CDK kinases, *Cell*. **146**(1):80-91.
- Homesley L, Lei M, Kawasaki Y, Sawyer S, Christensen T, and Tye BK. (2000), Mcm10 and the MCM2-7 complex interact to initiate DNA synthesis and to release replication factors from origins, *Genes Dev*.**14**:913-26
- Hook SS, Lin JJ and Dutta A (2007) Mechanisms to control rereplication and implications for cancer *Curr Opin Cell Biol.* **19**:663-71
- Izumi M, Yanagi K, Mizuno T, Yokoi M, Kawasaki Y, Moon KY, Hurwitz J, Yatagai F and Hanaoka F (2000) The human homolog of Saccharomyces cerevisiae Mcm10 interacts with replication factors and dissociates from nuclease-resistant nuclear structures in G(2) phase, *Nucleic Acids Res* **28:**769–477
- Izumi M, Yatagai F and Hanaoka F (2001) Cell cycle-dependent proteolysis

and phosphorylation of human Mcm10*, JBC* **276:**48526–48531

- Izumi M, Yatagai F and Hanaoka F (2004), Localization of human Mcm10 is spatially and temporally regulated during the S phase, *JBC* **279:**32569–32577
- Koepp DM (2010), The replication stress response and the ubiquitin system: a new link in maintaining genomic integrity. *Cell Div.* **5**:8
- Mizuno T, Yamagishi K, Miyazawa H, Hanaoka F. (1999), Molecular architecture of the mouse DNA polymerase alpha-primase complex, *Mol. Cell. Biol.* **19**:7886–96
- Nick McElhinny SA, Gordenin DA, Stith CM, Burgers PM, Kunkel TA (2008), Division of labor at the eukaryotic replication fork, *Mol Cell*.**30**(2):137-44
- Sclafani RA and Holzen TM (2007), Cell cycle regulation of DNA replication, *Annu Rev Genet* **41**:237–280
- Umar A and Kunkel TA (1996), DNA-replication fidelity, mismatch repair and genome instability in cancer cells *Eur. J. Biochem* **238**:297–307
- van Deursen F, Sengupta S, De Piccoli G, Sanchez-Diaz A, Labib K. (2012), Mcm10 associates with the loaded DNA helicase at replication origins and defines a novel step in its activation, *EMBO J.* **31**(9):2195-206.
- Williams GH and Stoeber K (2007), Cell cycle markers in clinical oncology, *Curr Opin Cell Biol*. **19:**672-9

Chapter 2

The mini-chromosome maintenance (Mcm)
complex interacts with
DNA polymerase α-primase
and stimulates
its ability to synthesize RNA primers

Introduction

2.1 - INTRODUCTION

In eukaryotic cells, the initiation of DNA replication proceeds in two steps: pre-replication complex (pre-RC) formation and its activation. At each step, the Mcm proteins play important roles: as a core component of the protein platform for replication initiation and as a key component of the helicase complex, which unwinds parental DNA for duplication of leading and lagging strands [Masai H et al. (2010)]. In vitro, DNA helicase activity was found to be associated with the Mcm4/6/7 complex but not with the Mcm2/3/4/5/6/7 (Mcm2~7) complex [Ishimi Y (1997), You Z et al. (1999), Kaplan DL et al. (2003), You Z & Masai H (2008)]. Previous works have shown that the Mcm2~7 complex associates with many other factors during the process of replication. It has been reported that the complex of Mcm2~7, Cdc45 and GINS (CMG complex) shows an efficient DNA helicase activity [Bochman ML & Schwacha A (2009), Ilves I et al. (2010)], leading to the suggestion that CMG is a functional form of the helicase machinery for eukaryotic DNA replication. Furthermore, Mcm10, Ctf4 (And-1), DNA polymerase α, DNA polymerase α-primase, Tof1-Csm3 (Tim-Tipin) and Mrc1 (Claspin), in addition to CMG, were found to generate a multi-molecular assembly in budding yeast [Gambus A et al. (2006), Gambus A et al. (2009)].

Mammalian DNA polymerase α-primase contains four subunits, p180, p68, p58, and p48 [Arezi B & Kuchta RD (2000), Kuchta RD & Stengel G (2010)]. The DNA polymerase activity resides in the p180 subunit, while the DNA primase activity requires the p58 and p48 subunits that are normally tightly associated with DNA polymerase α.DNA primase catalyzes the synthesis of short RNA oligomers used as primers for DNA synthesis. Primase nonspecifically binds to single-stranded DNA [Corn JE et al. (2008)]. Functional cooperation between DNA helicase and primase has been well studied in prokaryotic and viral systems. For examples, in Escherichia coli, the replicative DNA helicase DnaB stimulates the DnaG primase action on a naked single-stranded DNA [Arai K & Kornberg A (1979), Lu YB et al. (1996), Mitkova AV (2003)]. The primase was shown to stimulate the DnaB helicase activity [Wang G et al (2008), Bird LE et al (2000)]. The proposed architecture of the replication fork has provided insight into how

primase (DnaG)-helicase (DnaB) may interact with each other to facilitate their actions [Wang G et al (2008), Corn JE & Berger JM (2006), Bailey S et al. (2007)]. The model estimates that three molecules of primase bind to one DnaB hexamer. The primase may stabilize the conformation of the DnaB hexamer on DNA, resulting in more processive unwinding. On the other hand, DnaB may facilitate the recognition of target sites for DnaG primase action through its single-stranded DNA binding activity [Wang G et al (2008), Corn JE & Berger JM (2006), Patel SS et al. (2011)].

In T7 phage, a single protein (gp4) contains both primase and helicase activities on separate domains [Patel SS et al. (2011), Johnson DE et al. (2007), Stano NM et al. (2005), Pandey M et al. (2009)], which are related to bacterial DnaG and DnaB, respectively. At the replication fork, priming loop may be generated on the lagging strand through physical association between primase and helicase, resulting in more efficient DNA synthesis through coupling of DNA chain elongation and unwinding and easy handoff to the polymerase [Patel SS et al. (2011), Stano NM et al. (2005), Pandey M et al. (2009)]. The bacteriophage T4 primase (gp61) also binds tightly to the hexameric T4 helicase (gp41) to form a primosome complex, resulting in increased DNA priming activity [Hinton DM & Nossal NG (1987), Valentine AM et al. (2001), Yang J et al. (2005)].

During SV 40 replication, T antigen (Tag) physically binds to the DNA polymerase α-primase complex and stimulates its DNA primase and polymerase activities [Collins KL & Kelly TJ (1991), Schneider C et al. (1994), Weisshart K et al. (2000)]. Mouse DNA helicase B stimulates DNA primase-catalyzed synthesis probably through direct interaction [Saitoh A et al (1995)]. In addition, the Mcm complex stimulates RNA synthesis by the viral RNA polymerase complex [Kawaguchi A & Nagata K (2007)]. A protein containing homology to both eukaryotic DNA primase and Mcm was identified on a bacteriophage genome of the bacterium Bacillus cereus [McGeoch AT & Bell SD (2005)] and displayed not only helicase but also DNA primase and polymerase activities [Sanchez-Berrondo J et al. (2012)]. The presence of both helicase and primase motifs on one single polypeptide is reminiscent of the T7 phage primase-helicase protein. Thus, it is likely that the Mcm hexameric helicase also interacts with

DNA polymerases for coordinating unwinding and DNA chain elongation at the replication fork.

In this report, we have examined the physical and functional interactions of DNA polymerase α-primase with the Mcm complexes. We show that primer RNA synthesis by primase is stimulated by its interaction with the Mcm complexes.

Results

2.2 RESULTS

2.2.1. MCM FORMS A COMPLEX WITH THE DNA POLYMERASE A-PRIMASE OR DNA PRIMASE

The progression of replication fork requires the interaction of many proteins including the interaction of six Mcm subunits to form a hetero-hexameric complex [Masai H et al. (2010)]. In this report, we have explored the possibility that the Mcm helicase and the DNA polymerase α-primase physically and functionally interact with each other at the fork. Potential interaction between the mouse Mcm4/6/7 complex and mouse DNA polymerase α-primase tetrameric complex was explored by using glycerol gradient sedimentation. The Mcm4 and Mcm7 subunits co-sedimented with the p180 and p48 subunits at around the fraction 7, as shown by immunoblotting in Fig. 1, indicating that Mcm4/6/7 and DNA polymerase α-primase form a complex.

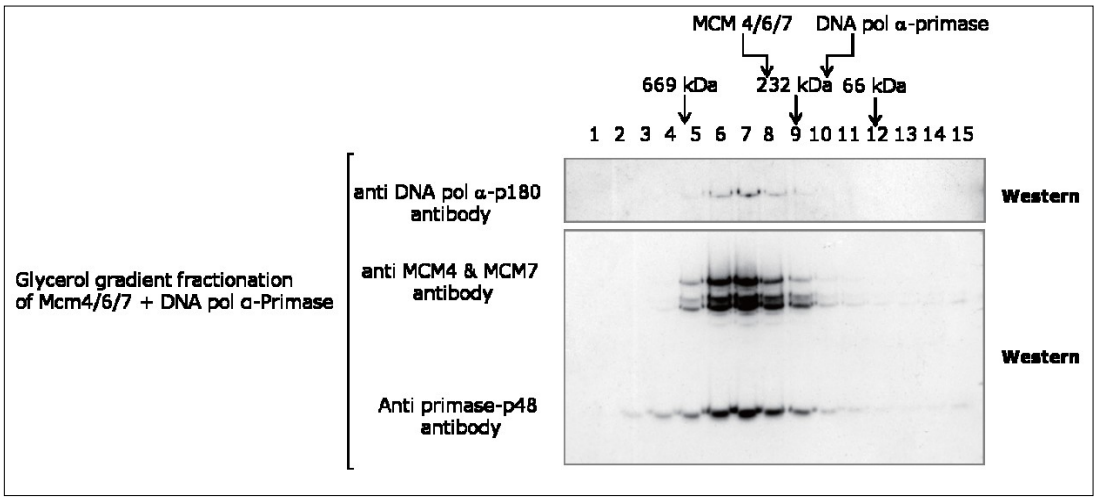

Figure 1. Complex formation of Mcm4/6/7 with DNA polymerase α-primase. Purified DNA polymerase α-primase and Mcm4/6/7 complexes were mixed and fractionated by centrifugation at 36,000 rpm for 16 h on a 15–30% glycerol gradient. Protein in each fraction was analyzed by 10% SDS-PAGE and immunoblotting using the indicated antibodies. The arrows indicate the positions of Mcm4/6/7 and DNA polymerase α-primase when loaded separately in the glycerol gradient. Thyroglobulin (669 kDa), catalase (232 kDa), lactate dehydrogenase (140 kDa), and albumin (66 kDa) (GE Healthcare) were used as protein molecular weight markers.

The Mcm4/6/7 complex alone peaked at around the fraction 8 while DNA polymerase α-primase elutes around fractions 10-11. Previous data shown that the Mcm4, Mcm6, and Mcm7 proteins co-sedimented and peaked between the protein

marker thyroglobulin (669 kDa) and catalase (232 kDa) in glycerol gradient centrifugation [You Z et al. (1999), You Z & Masai H (2008)]. The–DNA polymerase α-primase tetrameric complex co-sedimented at 9.1S between the catalase (232 kDa) and ADH (150 kDa) in glycerol gradient centrifugation in previous report [Mizuno T et al. (1999)]. This result suggests a possibility that Mcm4/6/7 forms a complex with DNA polymerase α-primase, although we cannot rule out the possibility of a distinct form of the Mcm4/6/7-DNA polymerase α-primase complex.

In order to further characterize the interaction between Mcm and primase, we investigated whether the Mcm2~7 hetero-hexamer could form a complex with primase (p48/p58). Mcm2~7 complex was purified from insect cells infected with recombinant baculoviruses. Physical interaction between the purified Mcm2~7 and p48/p58 protein complexes was examined by glycerol gradient centrifugation.

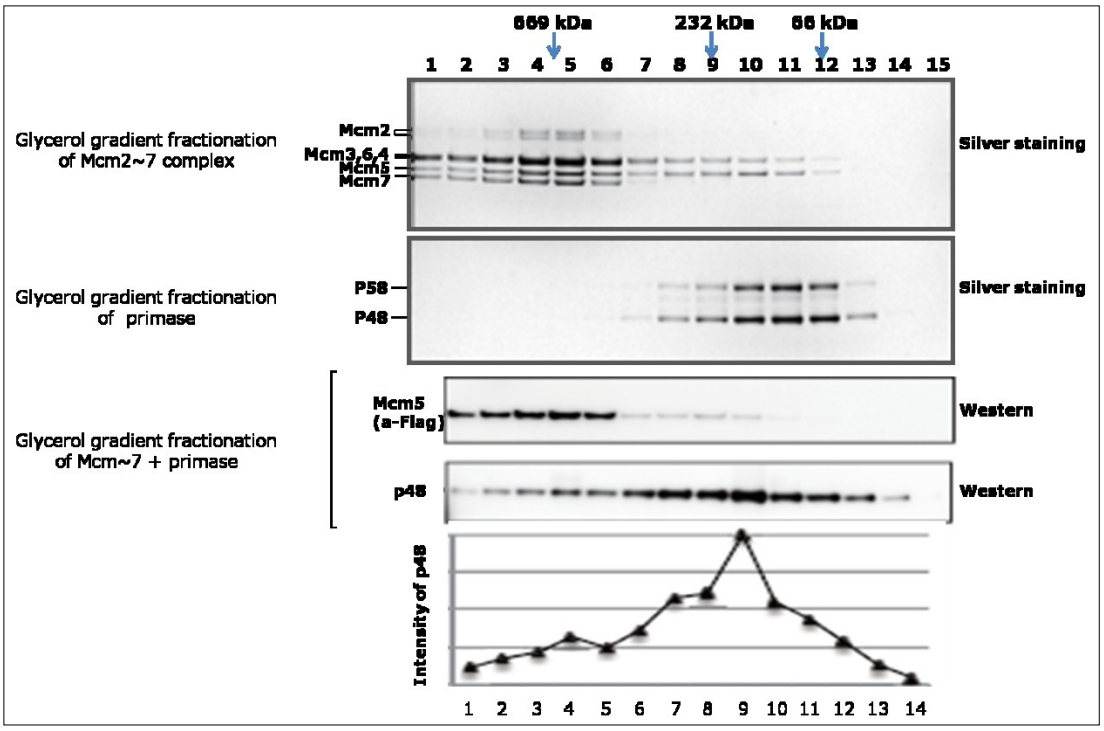

Figure 2. Complex formation of Mcm2~7 with DNA primase. Purified Mcm2~7 and primase complexes, singly (upper and middle panels) or in combination (bottom two panels), were fractionated by centrifugation at 36,000 rpm for 18 h on a 15–35% glycerol gradient in the presence of 1 mM ATP and each fraction was subjected to 4-20% SDSPAGE, followed by silver staining or western blotting. The positions of protein markers are indicated.
In the lowest graph, the amounts of p48 subunits of western-blotting in lower panels were quantified, and the levels relative to the maximum intensity of p48 (lane 10; taken as 100) are presented. Thyroglobulin (669 kDa), catalase (232 kDa), lactate dehydrogenase (140 kDa), and albumin (66 kDa) (GE Healthcare) were used as protein molecular weight markers.

The Mcm2~7 complex sedimented at around fractions 4–5 (first panel), consistent with the heterohexameric structure, as previously reported [You Z & Masai H (2008)]. The purified p48/p58 protein sedimented predominantly in the fractions 10–12, at a molecular weight of about 100 kDa (second panel).

When p48/p58 was mixed with Mcm2~7, a portion of p48 co-sedimented with the Mcm2~7 complex at fraction 5, as shown by a small peak in glycerol gradient centrifugation (the third and fourth panels and graph), suggesting that p48/p58 cosedimented with the Mcm2~7 complex. However, the majority of p48/p58 remained at low-molecular-weight position, suggesting that the interaction of Mcm2~7 and primase is unstable and that only a limited portion of primase formed a complex with Mcm2~7 at least under this experimental condition.

These results indicate that both Mcm4/6/7 and Mcm2~7 complexes associate with the hetero-dimeric primase complex.

2.2.2. PHYSICAL INTERACTIONS BETWEEN MCM AND PRIMASE

Immunoprecipitation experiments were conducted to investigate the interaction between the Mcm2~7 complex and DNA primase in the absence or presence of an oligonucleotide. Purified Mcm2~7 (containing the Flag-tagged Mcm5 protein)

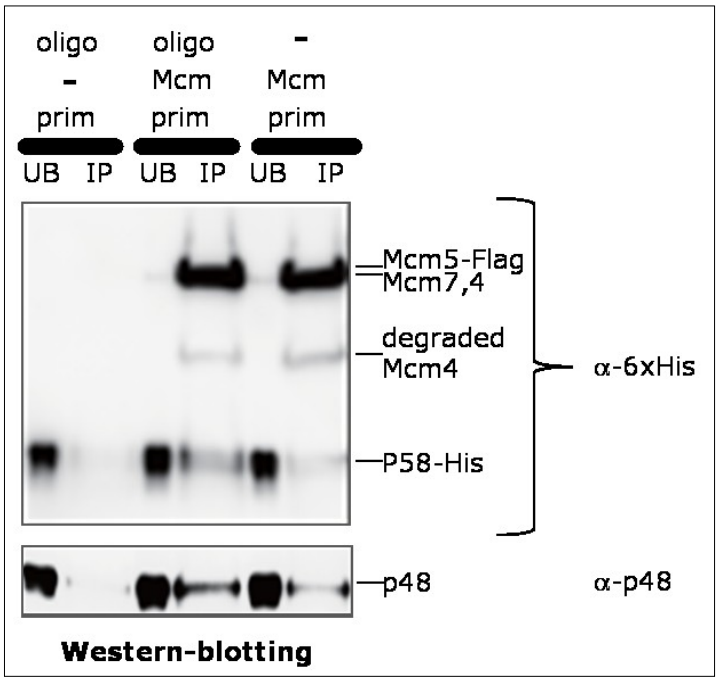

Figure 3. Direct interaction between Mcm helicase and primase. The purified Mcm2~7 complex (1 μg) was mixed with the His-tagged p48/p58 complex (0.25 μg) and immunoprecipitation was performed using anti-Flag M2 antibody beads (Sigma; Flag tag on Mcm5). The bound proteins were eluted with 0.1 M glycine (pH 2.8). For each sample, aliquots of the unbound and bound material were analyzed by immunoblotting using the indicated antibodies. Samples were run on 7.5% polyacrylamide gel.

and primase p48/p58 complexes were mixed with or without an oligonucleotide, and immunoprecipitation using anti-Flag antibody agarose beads were performed (Fig. 3).

Along with each Mcm subunit, p48 and p58 proteins were pulled down by the beads, detected by western-blotting, indicating that the Mcm helicase directly interacts with the primase complex. The amount of co-immuno-precipitated p48/p58 increased in the presence of DNA, suggesting that the interaction may be stabilized when DNA is present in the mixture.

In addition, we found that the p48 single subunit binds to Mcm2~7 in the absence of the oligonucleotide (Fig. 4). These data show that Mcm binds to primase through the p48 subunit in a manner independent from p180, p68 and DNA, and that this interaction is stabilized by DNA.

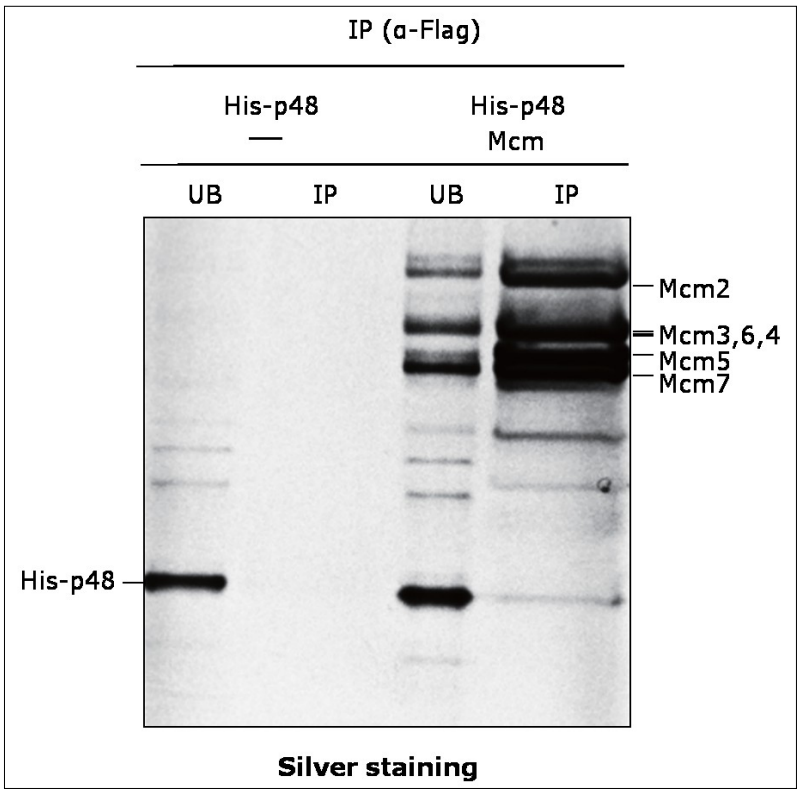

Figure 4. Mcm binds to DNA primase through the p48 subunit . The purified Mcm2~7 complex (1 μg) was mixed with His-p48 and immunoprecipitation was performed using anti-Flag M2 antibody beads (Sigma; Flag tag on Mcm5). The bound proteins were eluted with 0.1 M glycine (pH 2.8). The immunoprecipitate (IP) and 1/10 of unbound fractions (UB) were analyzed by silver staining. The heavy chain is visible in silver staining due to dissociation of the antibody from the beads.

To identify the subunits of Mcm interacting with primase, the human p48/p58-Flag hetero-dimeric complex and a single Mcm subunit was co-expressed in insect cells and

co-immunoprecipitation experiments were performed using the anti-Flag antibody agarose beads. The bound proteins were eluted from the resin by the Flag peptide. Mcm3, Mcm4 and Mcm7 but not Mcm2, 5, or 6 were co-immuno-precipitated with the human DNA primase (Fig. 5). Taken together, these results support a possibility that Mcm and primase can form a complex in cells.

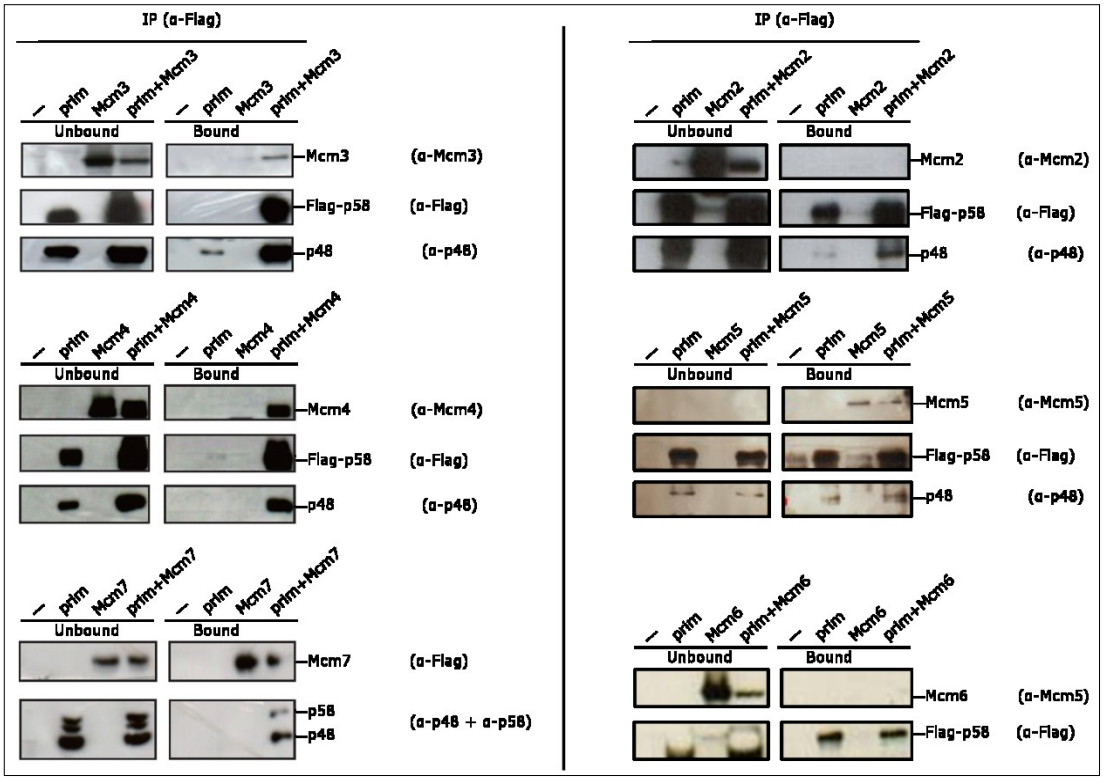

Figure 5. Direct interaction between Mcm helicase and primase Extracts of Sf9 insect cells expressing the subunits of human DNA primase (p48 and p58) and the indicated Mcm protein were subjected to immunoprecipitation analyses using anti-Flag agarose beads (GE Healthcare). The Flag tag was on Mcm7 in the lower-left panel and on p58 in all the others. Control experiments were carried out on extracts of cells expressing only the primase subunits or the indicated Mcm protein. Elution of bound proteins from the beads was carried out using a buffer containing the Flag peptide. For each sample, aliquots of the unbound and bound material were analyzed by immunoblotting using the indicated antibodies. Samples were run on 8%

2.2.3. INFLUENCE ON THE DNA-BINDING ACTIVITIES OF MCM4/6/7 AND PRIMASE

It has been known that Mcm4/6/7 binds to single-stranded DNA with a high affinity, but hardly binds to double-stranded DNA [You Z et al. (2003)]. In contrast, the Mcm2~7 complex exhibited very weak ssDNA binding in gel-shift

assay, while it showed ssDNA binding comparable to that by Mcm4/6/7 in filter binding assays [Bochman ML & Schwacha A (2007)]. This could be due to unstable association of Mcm2~7 with ssDNA. We examined DNA binding activities of the purified mouse Mcm4/6/7 and Mcm2~7. Consistent with previous studies, the Mcm2~7 complex showed very weak binding to ssDNA in the presence of the ATP-γ-S in mobility shift assays compared to Mcm4/6/7 complex (Fig. 6) [Bochman ML & Schwacha A (2007]. We next examined DNA-binding activities of the mouse Mcm4/6/7 and human p48/p58 complex using a 132-mer

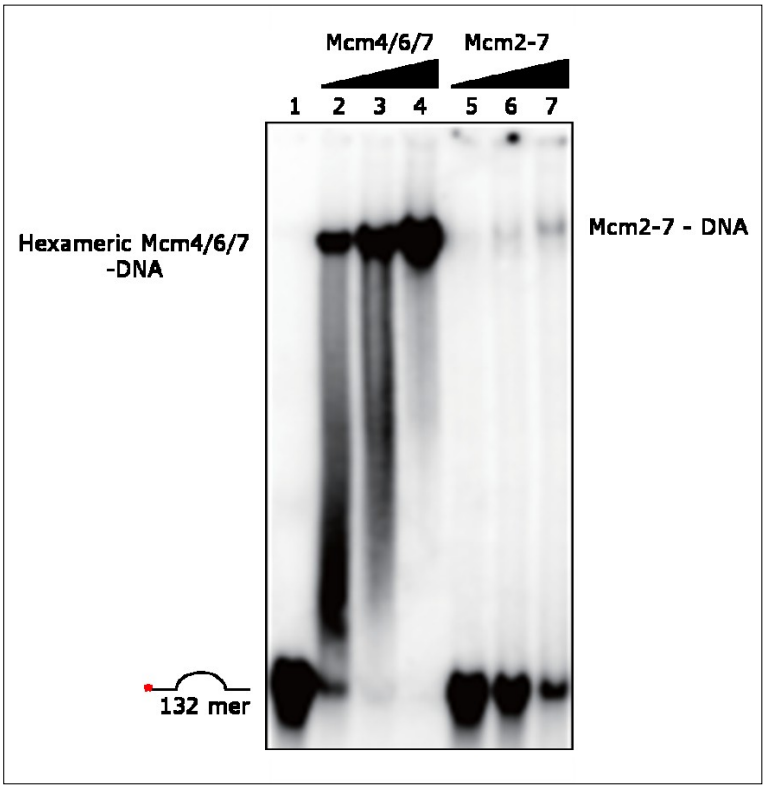

Figure 6. Effect of primase on the DNA-binding activity of Mcm4/6/7 and Mcm2~7. DNA-binding activities on ssDNA were examined in gel shift assays. The proteins added were; 37.5 ng (lane 2), 75 ng (lane 3) and 150 ng (lane 4) of Mcm4/6/7; 75 ng (lane 5), 150 ng (lane 6), and 300 ng (lane 7) of Mcm2~7. The reaction mixtures were incubated with 20 fmole substrate at 30 °C for 30 min, and were applied on a 5% native polyacrylamide gel

pyrimidine-rich oligonucleotide DNA that is known to be tightly bound by eukaryotic primase [Holmes AM et al. (1985)]. Strong ssDNA-binding activity was detected with primase. The binding of Mcm4/6/7 to the same ssDNA was not complete in this experiment due to the addition of a low amount of the protein (Fig. 7). In the presence of both primase and Mcm4/6/7, a band migrating slower than Mcm4/6/7 alone was detected and its intensity was proportional to the increasing concentrations of the primase (Fig. 7), suggesting the formation of a complex containing both Mcm4/6/7 and primase on single-stranded DNA

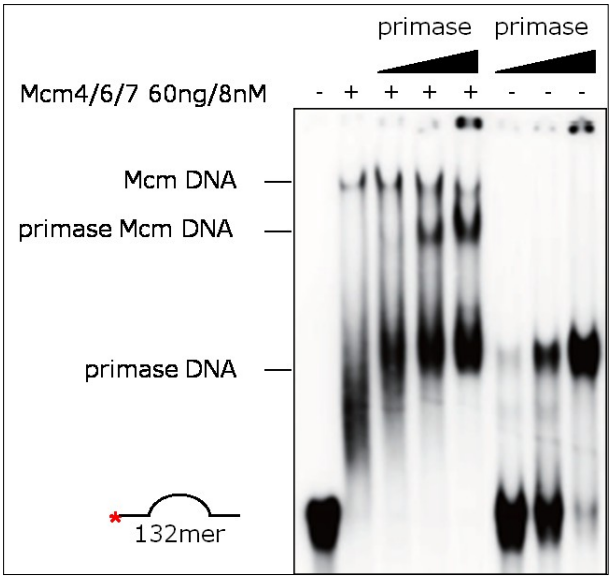

Figure 7. Effect of primase on the DNA-binding activity of Mcm4/6/7. Gel shift assays. A constant amount of Mcm4/6/7 (60 ng/ 8 nM, B) in the presence of various amounts of the p48/p58 primase was examined. The primase added were 30, 60, and 120 ng (25 nM, 50 nM and 100 nM respectively, as a monomer) The reaction mixtures were incubated with 20 fmole substrate at 30 °C for 30 min, and were applied on a 5% native polyacrylamide gel.

On the other hand, Mcm2~7 bound to ssDNA only inefficiently (Fig. 6), but this DNA binding activity increased in the presence of the primase (Fig. 8). The primase may stimulate the complex formation of Mcm with DNA through interaction with Mcm. Together, these results suggest that Mcm and primase interact on DNA and that the primase increases the association of Mcm with DNA.

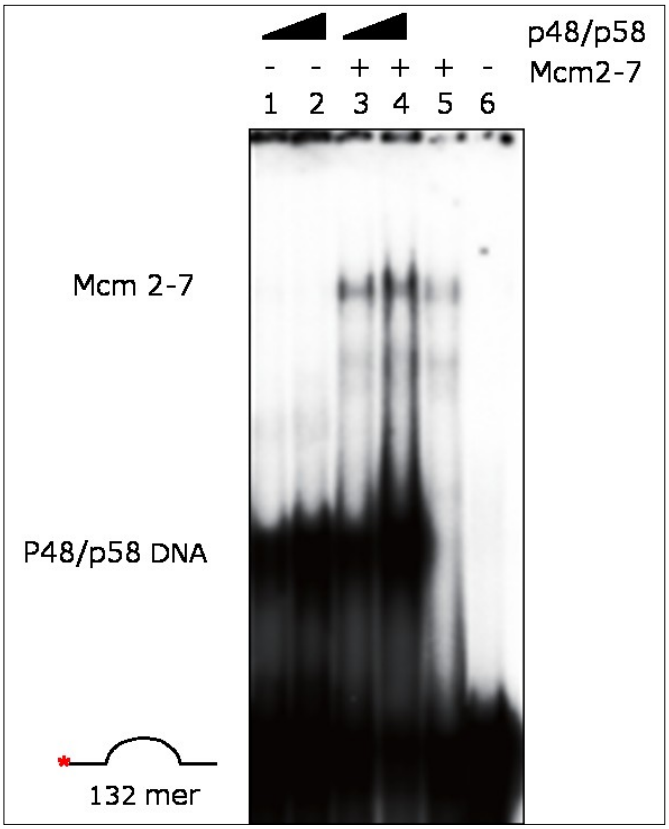

Figure 8. Effect of primase on the DNA-binding activity of Mcm2~7. A constant amount of Mcm2~7 (360 ng/ 50 nM) in the presence of various amounts (60 and 120 ng) of the p48/p58 primase was examined. The reaction mixtures were incubated with 20 fmole substrate at 30 °C for 30 min, and were applied on a 5% native polyacrylamide gel.

2.2.4. EFFECT OF PRIMASE ON MCM HELICASE AND ATPASE ACTIVITIES

To examine whether primase could affect the helicase activity of the Mcm complex, as demonstrated for DnaG primase and DnaB helicase in *E. coli.* [Wang G et al (2000),20], DNA helicase and ATPase activities of the Mcm4/6/7 were assayed in the presence of the p48/p58 primase. With a partial duplex substrate, the Mcm4/6/7 helicase activity was inhibited by the addition of increasing amounts of primase protein (Fig.9).

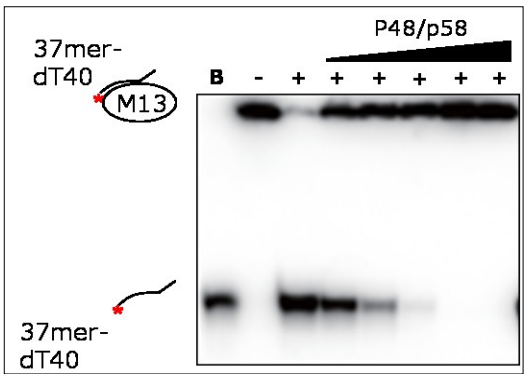

Figure 9. Effect of primase on DNA helicase activitiy of Mcm4/6/7. DNA helicase activities were examined with a constant amount (50 ng/7 nM) of Mcm4/6/7 and various amounts of primase using a partial heteroduplex substrate (10 fmole). The p48/p58 primase added were 30 ng, 60 ng, 120 ng, 240 ng and 480 ng. The samples were incubated at 37 ℃ for 1 hr and were then subjected to electrophoresis through a 10% polyacrylamide gel in 1x TBE buffer. B, boiled substrate DNA.

This inhibition is likely to have occurred due to substrate competition between Mcm and primase. In fact, addition of a 20-fold excess cold competitor oligonucleotide resulted in restoration of DNA unwinding activity by Mcm4/6/7 in the presence of the primase complex (Fig. 10).

Even under this condition, primase did not stimulate the helicase action of Mcm at any concentration tested. The reduced level of the displaced oligonucleotide at the highest concentration of p48/p58 is due to the binding of primase to the displaced oligonucleotide causing the mobility-shift. In fact, this mobility-shift disappeared when the reactions were treated extensivelywith proteinase K and SDS before being applied to the gel (data not shown).

DNA helicase activity depends on a set of sub-activities, including DNA binding and ATP hydrolysis and coordination of these activities is required to efficiently unwind DNA [Patel SS & Picha KM (2000]. The primase (p48/p58 complex) alone did not show any ATPase activity in the presence of single-stranded DNA

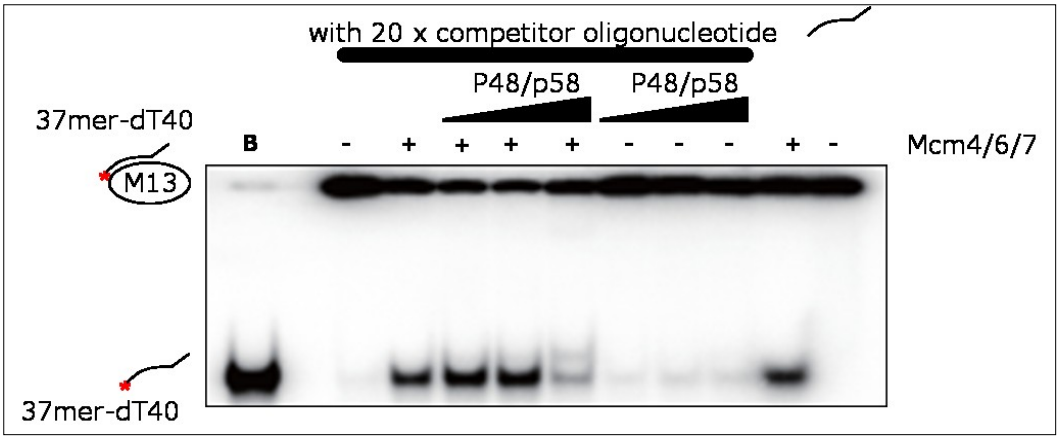

Figure 10. Effect of primase on DNA helicase of Mcm4/6/7. DNA helicase activity were examined with a constant amount (40 ng/5.6 nM) of Mcm4/6/7 and various amounts of primase using a partial heteroduplex substrate (10 fmole). 50 ng, 100 ng, and 200 ng of the p48/p58 primase were added. In the left group of assays 20-fold excess of cold competitor oligonucleotide DNA (37mer-dT_{40}) was also added. The samples were incubated at 37 ℃ for 1 hr and were then subjected to electrophoresis through a 10% polyacrylamide gel in 1x TBE buffer. B, boiled substrate DNA.

(Fig.11). Addition of primase (p48/p58 complex) did not increase the ATPase activity of Mcm, consistent with the absence of effect on the Mcm DNA helicase function

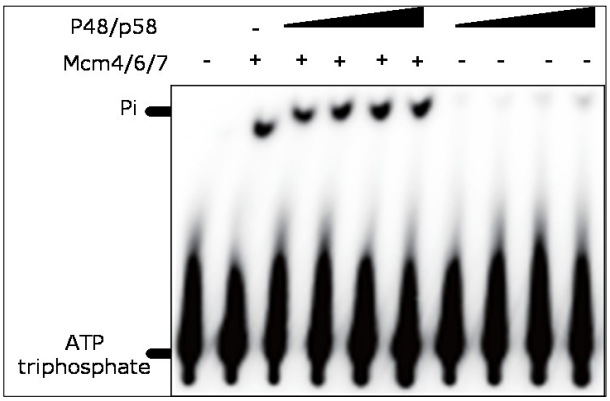

Figure 11. Effect of primase on ATP hydrolysis activity of Mcm4/6/7. ATPase activity of a constant amount of Mcm4/6/7 (150 ng) was measured in the presence of increasing amounts of p48/p58 primase (62.5 ng, 150 ng, 300 ng and 600 ng) and a 87 mer oligonucleotide (20 fmole). Pi, released phosphate.

2.2.5. MCM STIMULATES RNA PRIMER SYNTHESIS BY PRIMASE

Next, we examined whether the RNA primer synthesis would be affected by Mcm4/6/7 or Mcm2~7 complexes. We first observed that the RNA synthesis increased in proportion to the primase added (Fig.12A and 12B, lanes 2-3). In contrast, the Mcm4/6/7 and Mcm2~7 complexes by themselves did not show any RNA primer synthesis activity. Next, we examined the effect of addition of Mcm4/6/7 or Mcm2~7 on the primase synthesis function (Fig. 5A, lanes 4-7, and 5B, lanes 4-6). Both Mcm4/6/7 and Mcm2~7 stimulated primer synthesis by approximately three-fold. The Mcm complexes stimulated the primase activity of the hetero-tetrameric DNA polymerase α-primase complex as well (data not shown). However, Mcm did not have any effect on the DNA synthesis on a singly-primed M13mp18 single-stranded DNA template by DNA polymerase α-primase (data not shown).

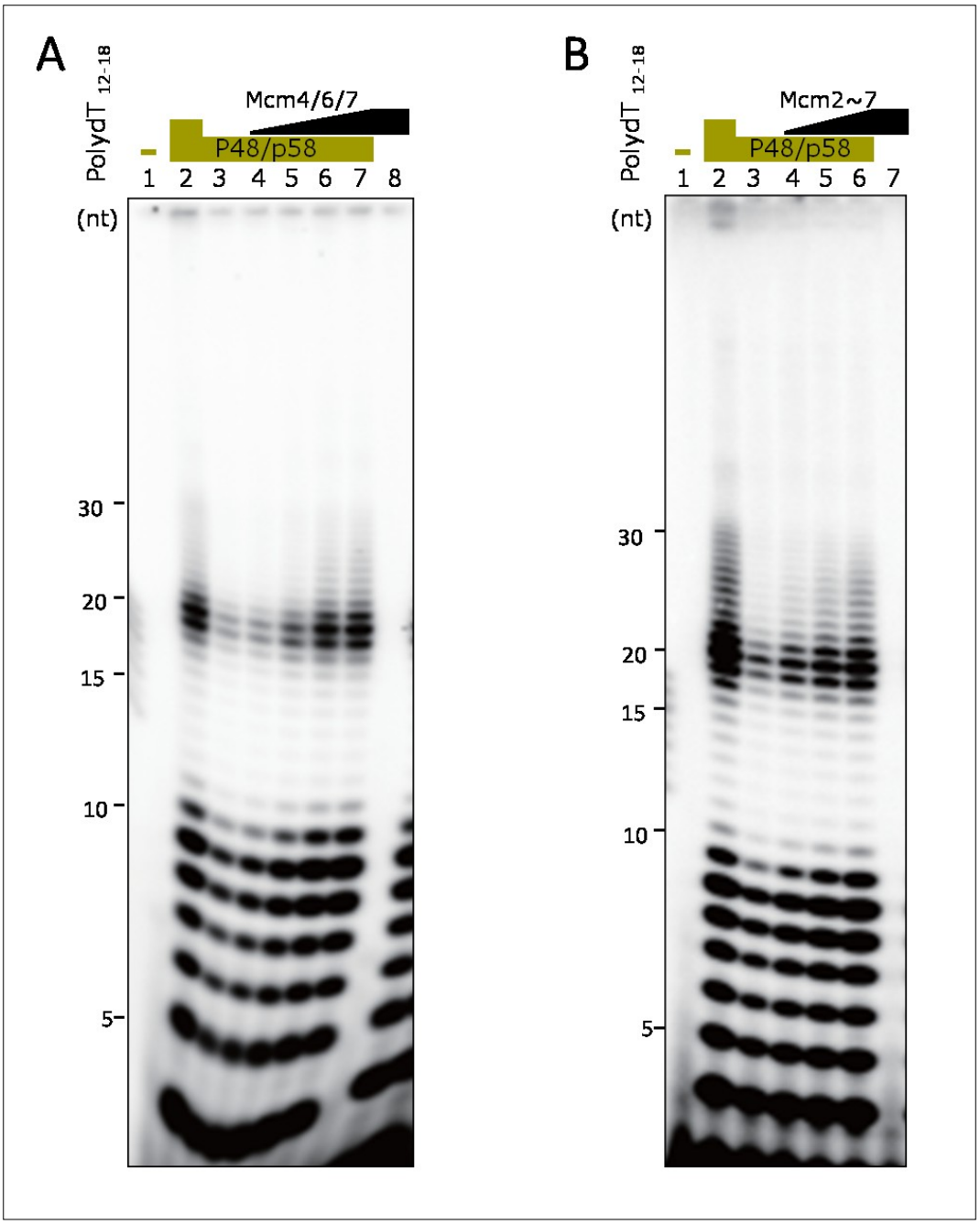

Figure 12. Stimulation of RNA primer synthesis by Mcm complexes. RNA primer was synthesized on poly(dT) by p48/p58 primase in the absence or presence of Mcm complex. After incubation for 1 hr at 37°C, the products were applied on 20% denaturing polyacrylamide gel in 1x TBE buffer. A labeled oligonucleotide (dT_{12-18}) was used as a size marker. (A) The proteins added were; 100 ng (lanes 3-7) and 300 ng (lane 2) of p48/58 primase; 100 ng (lane 4), 200 ng (lane 5), 400 ng (lane 6), and 600 ng (lanes 7 and 8) of Mcm4/6/7. (B) The proteins added were; 100 ng (lanes 3-6) and 300 ng (lane 2) of p48/58 primase; 100 ng (lane 4), 200 ng (lane 5) and 400 ng (lanes 6 and 7) of Mcm2~7.

Discussion

2.3 DISCUSSION

Physical and functional interaction between the replicative helicase and primase has been well known in bacteria and bacteriophages. We show here for the first time that the Mcm helicase forms a complex with DNA polymerase α-primase through direct interaction with the primase subunits. We also show that the primase activity is stimulated by the Mcm complexes. In the prokaryotic and animal viral replisome, physical links between DNA helicase, DNA polymerase and primase regulate fork progression and allow unwinding to be coordinated with DNA chain elongation [Arezi B & Kuchta RD (2000), Kuchta RD & Stengel G (2010), Patel SS et al. (2011)]. Our findings suggest a possibility that similar mechanisms may operate for the eukaryotic replisome (Fig. 7).

It was proposed that DnaB helicase activates DnaG primase by serving as a docking station to increase the local concentration of single-stranded DNA template relative to primase [Corn JE & Berger JM (2006)]. We have shown that Mcm forms a complex with DNA polymerase α-primase (Fig. 1-5) and this complex can bind to single-stranded DNA in gel-shift assays, probably through interaction between p48 and Mcm3/Mcm4/Mcm7 subunits (Fig. 4 and 5). It has been known that DNA polymerase α holoenzyme interacts with a Mcm subunit [Thommes P et al. (1992)]. As shown in Fig. 1, almost all the Mcm4/6/7 complex co-sedimented with the DNA polymerse α-primase complex. In contrast, only a portion of the primase polypeptide cosedimented with the Mcm2~7 complex (Fig.2). The polymerase subunits may facilitate the interaction between DNA polymerse α-primase and Mcm.

Primase stimulates Mcm ssDNA-binding activity (Fig. 6-8), suggesting that they cooperate with each other to facilitate fork progression and DNA chain elongation. The increase of Mcm2~7 with primase on DNA is less than expected that probably due to a transient or destabilized of interaction of Mcm2~7 complex with DNA. Indeed RNA primer synthesis is stimulated significantly by both the helicase-active Mcm4/6/7 and helicase-inactive Mcm2~7 complexes (Fig. 12). Thus, interactions between Mcm and primase, not the helicase activity of Mcm, may be important for stimulation of the priming activity. This is similar to the

previous report that a helicase-dead DnaB can stimulate DnaG primase [Shrimankar P et al. (1992)].

Mcm is a 3' to 5' helicase present on the leading strand [Ishimi Y (1997), You Z et al (1999), Kaplan DL et al. (2003), Bochman ML & Schwacha A (2009)], and thus, it needs to interact with the primase acting on the other strand [Ricke RM & Bielinsky AK (2004)]. It has been known that the eukaryotic polymerase and primase are associated with each in a highly flexible manner [Nunez-Ramirez R et al. (2011)]. The primase could interact with different surfaces of polymerase, potentially giving rise to a flexible movement in association with the moving polymerase. Thus, it is conceivable that primase present on the lagging strand interacts with the Mcm complex on the leading strand. Since the interaction between Mcm2~7 and primase is weak, it could be a transient or unstable association. We have not found in our *in vitro* assays any stimulatory effect of Mcm on the DNA synthesis catalyzed by the DNA polymerase α-primase complex. In contrast, the SV40 T-antigen helicase interacts with all four subunits of the polymerase α-primase complex and can stimulate both primase and DNA chain elongation activities of DNA polymerase α-primase complex [Collins KL & Kelly TJ (1991), Schneider C et al. (1994), Weisshart K et al. (2000)]. The failure of Mcm to stimulate DNA synthesis by DNA polymerase α *in vitro* may suggest that other replication fork proteins may be required for full stimulation of DNA chain elongation. In fact, a large replisome progression complex (RPC) containing GINS, Mcm, Cdc45, Mrc1, Tof1-Csm3, FACT, Ctf4/And-1, Mcm10 and DNA topoisomerase I was detected in budding yeast [Gambus A et al. (2006), Gambus A et al. (2009), Zhu W et al.(2007)]. It was reported that the GINS-Ctf4 complex of the RPC is crucial to couple Mcm2~7 to DNA polymerase α [Gambus A et al. (2009)]. Additional factors, such as Mcm10, GINS and Cdc45, are also known to bind to DNA polymerase α at the replication fork [Gambus A et al. (2006), De Falco et al (2007), Zhu W et al.(2007), Mimura S &, Takisawa H (1998)]. More recently, studies in yeasts indicated a role of Mcm10 in activation of the CMG helicase [Kanke M et al. (2012), van Deursen F et al.(2012)]. Effects of these factors on priming and DNA

synthesis activities of DNA polymerase α-primase need to be carefully examined in the future.

Our binding assays show that primase directly interacts with the Mcm3, 7, and 4 subunits (Fig. 5), which constitute a half surface of the hexameric Mcm ring. The helicase complex may be able to couple the helicase action on the leading strand and primer RNA synthesis on the lagging strand.

Our results suggest that Mcm forms a specific complex with DNA polymerase α-primase at the replication fork and that this interaction may facilitate RNA primer synthesis on the lagging strand (Fig. 7).

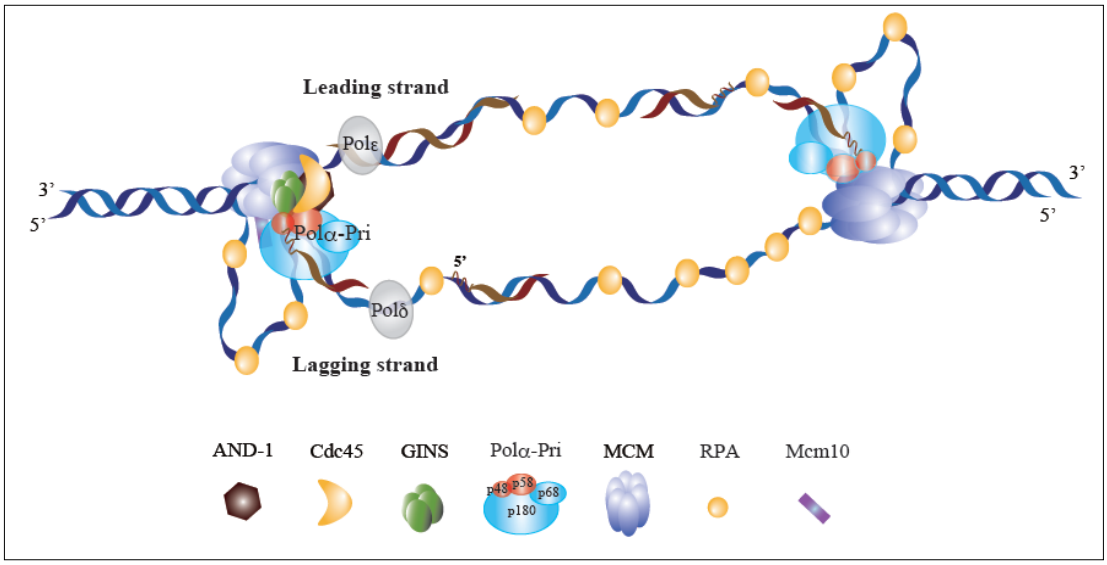

Figure 7. A model on coupling of Mcm helicase and primase at the replication fork for the lagging strand synthesis. When the primase synthesizes primers on the lagging strand template, its action may be coupled to the Mcm helicase present on the leading strand template through direct interaction. This may also increase the efficiency by which DNA polymerase a elongates the RNA primers.

This probably represents only a portion of the many protein-protein interactions which occur within the replisome complex. We propose that Mcm, moving on the leading strand, serves as a part of the bridge that links DNA polymerase α-primase so that primer synthesis occurs efficiently on the lagging strand. Our results also suggest the conservation of helicase-primase interaction at both prokaryotic and eukaryotic replication forks. The Mcm-polymerase α-primase assembly may operate in a manner analogous to many prokaryotic systems, such as *E. coli* chromosome, bacteriophage T7 and T4 [Corn JE &

Berger JM (2006), Patel SS et al. (2011), Pandey M et al. (2009), Yang J et al.(2005), Manosas M et al. (2009)]. Besides, it was recently reported that *Bacillus cereus* Mcm contains intrinsic primase and polymerase activities in addition to the helicase function [Sanchez-Berrondo J et al. (2012)]. Future analyses carried out with the helicase-proficient CMG complex, as well as other associated fork factors, will provide further insight into the functional and physical interactions that underpin the molecular functions of the highly efficient and versatile eukaryotic replisome complex.

Materials

&

Methods

2.4 MATERIALS AND METHODS

2.4.1. EXPRESSION AND PURIFICATION OF RECOMBINANT PROTEINS IN INSECT CELLS AND *E. COLI*

The highly purified recombinant Mcm4/6/7 and Mcm2~7 protein complexes were prepared from insect cells as follows. For expression of the Mcm4/6/7, HighFive cells were co-infected with recombinant baculoviruses expressing the His_6-Mcm4/Mcm6 proteins and those expressing the Mcm7-Flag, and were collected at 48 hr post-infection. The recombinant Mcm4/6/7 complex was purified as previously described [You Z et al. (2003)]. For expression of the Mcm2~7 complex, Sf9 or High Five cells were co-infected with the combination of Mcm2-Mcm7-His_6, Mcm4-His_6-Mcm6, and Mcm3-Mcm5-His_6-Flag baculoviruses, and were collected at 48 hr post-infection. The Mcm2~7 complex was purified with consecutive steps involving nickel-agarose affinity chromatography, anti-Flag M2 antibody agarose affinity chromatography and glycerol gradient sedimentation. Sf9 and High Five insect cells were cultured at 27 °C in Sf-900 II SFM (Life Technologies, Inc.) and EX-CELL 405 medium (JRH Biosciences), respectively.

His-tagged p58 and non-tagged p48 complex was over-produced in the *E. coli* BL21 (DE3) RIL strain and purified as previously described [Schneider A et al (1998)].

2.4.2. REAGENTS

Labeled and unlabeled dNTPs/rNTPs were purchased from GE Healthcare. M13mp18 single-stranded circular DNA (ssDNA) and T4 polynucleotide kinase (T4 PNK) were from TAKARA, and anti-Flag M2 antibody-agarose beads and Flag peptide were from Sigma. Oligonucleotides were purchased from Hokkaido System Science Co., Ltd. (Hokkaido, Japan).

2.4.3. CONSTRUCTION OF DNA SUBSTRATES

5'-tailed partial hetero-duplex substrates were constructed by annealing a dT_{40}-37mer oligonucleotide to M13mp18 ssDNA. The oligonucleotide carrying the 40mer oligo (dT) tail at the 3' end of the hybridizing 37mer sequence was first

labeled with [γ-^{32}P]ATP and T_4 PNK, and then annealed to M13mp18 ssDNA. The reaction mixture was heated at 95 °C, kept at 67 °C for 1 hr, and then allowed to slowly cool down to 30 °C. The labeled substrates were purified by Sepharose CL4B column chromatography (GE Healthcare). The 132mer oligonucleotide (5'-CCACACATGATTTGTTTGCTCCCTGAAATGATCTATATTTAATATATAA TGTATATTCCCTCGGGATTTTTTATTTTGTGTTATTCCACGGCATGAAA AACAAAAAACATTCTTCTCATCCTTGGTCCCTCA-3') was labeled with [γ-^{32}P]ATP and T_4 PNK. The Y-fork substrate was composed of a 50 nucleotide duplex region and a 30-mer or 60-meroligo (dT) sequence as the 5'or a 3' tail, respectively [You Z et al. (2003)]. The double-stranded DNA (173 bp) was labeled by filling in the cohesive ends with [α–^{32}P]dCTP and the Kleenow fragment of DNA polymerase I.

2.4.4. PRIMER RNA SYNTHESIS ASSAYS.

Primer RNA synthesis was carried out using poly(dT) or M13 ssDNA as templates. The assays (25 μl) contained 20 mM Tris-HCl (pH 7.5), 10 mM magnesium acetate, 5 mM dithiothreitol (DTT), and 0.1 mg/ml bovine serum albumin (BSA). The reaction mixtures with poly(dT) (2 nmole as nucleotide) contained 0.1 mM [α-^{32}P]ATP (3 μCi/nmol), whereas the mixtures with M13mp18 ssDNA (0.5 nmole as nucleotide) contained 200 μM ATP, 200 μM CTP, 200 μM UTP, 20 μM GTP and 0.125 μCi [α-^{32}P]GTP. After addition of 100-300 ng of primase, as indicated, assays were incubated for 1 hr at 37 °C. The products were ethanol-precipitated in the presence of 2.5 μl of 3 M sodium acetate (pH 5.2) and 10 μg of *E. coli* tRNA, washed with 75% ethanol, dried, re-suspended in a solution containing 80% deionized formamide, 5 mM ethylenediaminetetraacetic acid (EDTA) and 0.05% bromophenol blue. Primer RNAs were analyzed on denaturing polyacrylamide gel electrophoresis. Samples were heated at 95 °C for 3 min and were loaded onto 20% polyacrylamide gel (acrylamide: bisacrylamide ratio, 19:1) containing 7 M urea and 0.5 x Tris-Borate-EDTA (TBE) buffer. As a molecular weight marker, labeled oligo(dT_{12-18}), 10-bp DNA ladder, and 50-bp DNA ladder were used.

2.4.5. DNA-BINDING AND HELICASE ASSAYS

DNA helicase and DNA-binding activities were examined in reaction mixtures (12 μl) containing 25 mM Tris-HCl (pH 7.5), 40 mM sodium acetate, 10 mM magnesium acetate, 20 mM 2-mercaptoethnol, 0.25 mg/ml BSA, 0.5 mM ATP-γ-S, and various labeled substrates (20 fmole for DNA binding and 10 fmole for helicase assays). In DNA binding assays, complexes were separated on a 5% native polyacrylamide gel after incubation at 30 °C for 30 min. In DNA helicase assay, after incubation of the above reaction mixtures at 30 °C for 30 min, ATP (final 10 mM) was added and incubation was continued at 37 °C for 30 min. After termination of the reaction by the addition of stop buffer (final 20 mM EDTA and 0.1% sodium dodecylsulphate [SDS]), the samples were separated on a non-denaturing polyacrylamide gel in 1 x TBE buffer.

2.4.6. ATPASE ASSAYS

ATPase activities were examined in reaction mixtures (12 μl) containing 50 mM Tris-HCl (pH 7.5), 10 mM magnesium acetate, 20 mM 2-mercaptoethnol, 0.5 mg/ml BSA, 1 mM ATP (with 2 μCi of [γ-^{32}P]ATP), and 87mer oligonucleotide (20 pmole). After incubation at 30 °C for 1 hr, aliquots were spotted onto a polyethyleneimine-cellulose thin layer plate, and ATP and Pi were separated by chromatography in 1 M formic acid and 0.5 M LiCl. The radioactivity on the plate was detected by using a Bio-Image analyzer (BAS 2500; Fuji).

2.4.7. IMMUNO-PRECIPITATION (IP) ANALYSES

The primase (His-p58/p48 complex) was mixed with purified Mcm2~7 containing a Flag-tag in Mcm5 and immunoprecipitation were performed using anti-Flag M2 antibody agarose beads (Sigma). The pre-washed anti-Flag antibody beads were mixed with the proteins with or without an oligonucleotide in a buffer containing 50 mM Tris-HCl (pH 7.5), 100 mM sodium acetate, 5 mM magnesium acetate, 1 mM ATP, 10% glycerol, and 0.01% Triton-X-100. After a 2-hr incubation at 4 °C, beads were washed three times with the same buffer and bound proteins were eluted with 0.1 M glycine (pH 2.8) twice. The eluted samples were analyzed by

SDS-polyacrylamide gel electrophoresis (PAGE) followed by silver staining or western-blotting with anti-penta-His antibody (Qiagen) or anti-p48 antibody.

2.4.8. IMMUNOPRECIPITATION EXPERIMENTS ON INSECT CELLS CO-INFECTED WITH BACULOVIRUSES

Sf9 cells were seeded at 5×10^6 in 10 cm dishes, infected with appropriate baculoviruses and incubated at 27 °C. At 72 hrs after infection cells were harvested, centrifuged at 1000−g for 5 min and cell pellets were re-suspended in the lysis buffer (40 mM HEPES-NaOH, pH 7.5, 100 mM sodium acetate, 1 mM DTT, 10 mM magnesium acetate, 1 mM EDTA, 0.1% NP-40, protease and phosphatase inhibitors tablets [Roche]). Cells were lysed using a Soniprep 150 (Sanyo) at 10 amplitude microns, four times for 10 sec each. One tenth of the supernatant was mixed with 10 μl of M2 Flag-Agarose affinity gel. Samples were washed five times with the lysis buffer and eluted with the lysis buffer containing 0.3 mg/ml of Flag peptide. One fifth of the immunoprecipitates were loaded on SDS-PAGE, blotted and detected with anti-Flag or other antibodies indicated.

2.4.9. GLYCEROL GRADIENT FRACTIONATION

Purified Mcm4/6/7 complex alone or the mixtures of DNA polymerase α-primase and Mcm4/6/7 complexes were loaded onto a 15-30% glycerol gradient in 20 mM Tris-HCl (pH 7.5), 150 mM NaCl, 0.5 mM EDTA, 1 mM DTT, 0.01% Triton X-100, and 0.1 mM phenylmethylsulfonyl fluoride (PMSF). Since protein concentration of both polymerase and Mcm was low, heat-denatured α-Casein (10 μg; from Sigma) was added for stabilization. After centrifugation at 36,000 rpm in a TLS-55 rotor for 16 hrs at 4° C, 15 fractions were collected from the top of the gradient. Purified Mcm2~7 complex and human DNA primase, singly or in combination, were fractionated in a 15-35% glycerol gradient in 20 mM Tris-HCl (pH 7.5), 100 mM NaCl, 1 mM ATP, 5 mM magnesium acetate, 0.5 mM EDTA, 1 mM DTT, 0.01% Triton X-100, and 0.1 mM PMSF at 36,000 rpm in a TLS-55 rotor for 18 hrs at 4° C.

References

2.5. REFERENCES

- Arai K, Kornberg A (1979) A general priming system employing only dnaB protein and primase for DNA replication. Proc Natl Acad Sci U S A 76: 4308-4312.
- Arai K, Kornberg A (1981) Mechanism of dnaB protein action. III. Allosteric role of ATP in the alteration of DNA structure by dnaB protein in priming replication. J Biol Chem 256: 5260-5266.
- Arezi B, Kuchta RD (2000) Eukaryotic DNA primase. Trends Biochem Sci 25: 572-576.
- Bailey S, Eliason WK, Steitz TA (2007) Structure of hexameric DnaB helicase and its complex with a domain of DnaG primase. Science 318: 459-463.
- Bird LE, Pan H, Soultanas P, Wigley DB (2000) Mapping protein-protein interactions within a stable complex of DNA primase and DnaB helicase from Bacillus stearothermophilus. Biochemistry 39: 171-182.
- Bochman ML, Schwacha A (2007) Differences in the single-stranded DNA binding activities of MCM2-7 and MCM467: MCM2 and MCM5 define a slow ATP-dependent step. J Biol Chem 282: 33795-33804.
- Bochman ML, Schwacha A (2009) The Mcm complex: unwinding the mechanism of a replicative helicase. Microbiol Mol Biol Rev 73: 652-683.
- Collins KL, Kelly TJ (1991) Effects of T antigen and replication protein A on the initiation of DNA synthesis by DNA polymerase alpha-primase. Mol Cell Biol 11: 2108-2115.
- Corn JE, Berger JM (2006) Regulation of bacterial priming and daughter strand synthesis through helicase-primase interactions. Nucleic Acids Res 34: 4082-4088.
- Corn JE, Pelton JG, Berger JM (2008) Identification of a DNA primase template tracking site redefines the geometry of primer synthesis. Nat Struct Mol Biol 15: 163-169.
- Costa A, Ilves I, Tamberg N, Petojevic T, Nogales E, et al. (2011) The structural basis for MCM2-7 helicase activation by GINS and Cdc45. Nat Struct Mol Biol 18: 471-477.

- De Falco M, Ferrari E, De Felice M, Rossi M, Hubscher U, et al. (2007) The human GINS complex binds to and specifically stimulates human DNA polymerase alpha-primase. EMBO Rep 8: 99-103.
- Frick DN, Richardson CC (2001) DNA primases. Annu Rev Biochem 70: 39-80.Gambus A, Jones RC, Sanchez-Diaz A, Kanemaki M, van Deursen F, et al. (2006) GINS maintains association of Cdc45 with MCM in replisome progression complexes at eukaryotic DNA replication forks. Nat Cell Biol 8: 358-366.
- Gambus A, van Deursen F, Polychronopoulos D, Foltman M, Jones RC, et al. (2009) A key role for Ctf4 in coupling the MCM2-7 helicase to DNA polymerase alpha within the eukaryotic replisome. Embo J 28: 2992-3004
- Hinton DM, Nossal NG (1987) Bacteriophage T4 DNA primase-helicase. Characterization of oligomer synthesis by T4 61 protein alone and in conjunction with T4 41 protein. J Biol Chem 262: 10873-10878.
- Holmes AM, Cheriathundam E, Bollum FJ, Chang LM (1985) Initiation of DNA synthesis by the calf thymus DNA polymerase-primase complex. J Biol Chem 260: 10840-10846.
- Ilves I, Petojevic T, Pesavento JJ, Botchan MR (2010) Activation of the MCM2-7 Helicase by Association with Cdc45 and GINS Proteins. Mol Cell 37: 247-258.
- Ishimi Y (1997) A DNA helicase activity is associated with an MCM4, -6, and -7 protein complex. J Biol Chem 272: 24508-24513.
- Johnson DE, Takahashi M, Hamdan SM, Lee SJ, Richardson CC (2007) Exchange of DNA polymerases at the replication fork of bacteriophage T7. Proc Natl Acad Sci U S A 104: 5312-5317.
- Kanke M, Kodama Y, Takahashi TS, Nakagawa T, Masukata H (2012) Mcm10 plays an essential role in origin DNA unwinding after loading of the CMG components. EMBO J 31: 2182-2194.
- Kaplan DL, Davey MJ, O'Donnell M (2003) Mcm4,6,7 uses a "pump in ring" mechanism to unwind DNA by steric exclusion and actively translocate along a duplex. J Biol Chem 278: 49171-49182.
- Kawaguchi A, Nagata K (2007) De novo replication of the influenza virus

RNA genome is regulated by DNA replicative helicase, MCM. EMBO J 26: 4566-4575.

- Kuchta RD, Stengel G (2010) Mechanism and evolution of DNA primases. Biochim Biophys Acta 1804: 1180-1189
- Kukimoto I, Igaki H, Kanda T (1999) Human CDC45 protein binds to minichromosome maintenance 7 protein and the p70 subunit of DNA polymerase alpha. Eur J Biochem 265: 936-943.
- Lu YB, Ratnakar PV, Mohanty BK, Bastia D (1996) Direct physical interaction between DnaG primase and DnaB helicase of Escherichia coli is necessary for optimal synthesis of primer RNA. Proc Natl Acad Sci U S A 93: 12902-12907.
- Manosas M, Spiering MM, Zhuang Z, Benkovic SJ, Croquette V (2009) Coupling DNA unwinding activity with primer synthesis in the bacteriophage T4 primosome. Nat Chem Biol 5: 904-912.
- Masai H, Matsumoto S, You Z, Yoshizawa-Sugata N, Oda M (2010) Eukaryotic chromosome DNA replication: where, when, and how? Annu Rev Biochem 79: 89-130.
- McGeoch AT, Bell SD (2005) Eukaryotic/archaeal primase and MCM proteins encoded in a bacteriophage genome. Cell 120: 167-168.
- Mimura S, Takisawa H (1998) Xenopus Cdc45-dependent loading of DNA polymerase alpha onto chromatin under the control of S-phase Cdk. Embo J 17: 5699-5707.
- Mitkova AV, Khopde SM, Biswas SB (2003) Mechanism and stoichiometry of interaction of DnaG primase with DnaB helicase of Escherichia coli in RNA primer synthesis. J Biol Chem 278: 52253-52261.
- Mizuno T, Yamagishi K, Miyazawa H, Hanaoka F (1999) Molecular architecture of the mouse DNA polymerase alpha-primase complex. Mol Cell Biol 19: 7886-7896.
- Nunez-Ramirez R, Klinge S, Sauguet L, Melero R, Recuero-Checa MA, et al. (2011) Flexible tethering of primase and DNA Pol alpha in the eukaryotic primosome. Nucleic Acids Res 39: 8187-8199.
- Pandey M, Syed S, Donmez I, Patel G, Ha T, et al. (2009) Coordinating DNA replication by means of priming loop and differential synthesis rate. Nature

462: 940-943.

- Patel SS, Picha KM (2000) Structure and function of hexameric helicases. Annu Rev Biochem 69: 651-697.
- Patel SS, Pandey M, Nandakumar D (2011) Dynamic coupling between the motors of DNA replication: hexameric helicase, DNA polymerase, and primase. Curr Opin Chem Biol 15: 595-605.
- Ricke RM, Bielinsky AK (2004) Mcm10 regulates the stability and chromatin association of DNA polymerase-alpha. Mol Cell 16: 173-185.
- Saitoh A, Tada S, Katada T, Enomoto T (1995) Stimulation of mouse DNA primase-catalyzed oligoribonucleotide synthesis by mouse DNA helicase B. Nucleic Acids Res 23: 2014-2018.
- Sanchez-Berrondo J, Mesa P, Ibarra A, Martinez-Jimenez MI, Blanco L, et al. (2012) Molecular architecture of a multifunctional MCM complex. Nucleic Acids Res 40: 1366-1380.
- Schneider A, Smith RW, Kautz AR, Weisshart K, Grosse F, et al. (1998) Primase activity of human DNA polymerase alpha-primase. Divalent cations stabilize the enzyme activity of the p48 subunit. J Biol Chem 273: 21608-21615.
- Schneider C, Weisshart K, Guarino LA, Dornreiter I, Fanning E (1994) Species-specific functional interactions of DNA polymerase alpha-primase with simian virus 40 (SV40) T antigen require SV40 origin DNA. Mol Cell Biol 14: 3176-3185.
- Shrimankar P, Stordal L, Maurer R (1992) Purification and characterization of a mutant DnaB protein specifically defective in ATP hydrolysis. J Bacteriol 174: 7689-7696.
- Stano NM, Jeong YJ, Donmez I, Tummalapalli P, Levin MK, et al. (2005) DNA synthesis provides the driving force to accelerate DNA unwinding by a helicase. Nature 435: 370-373.
- Thommes P, Fett R, Schray B, Burkhart R, Barnes M, et al. (1992) Properties of the nuclear P1 protein, a mammalian homologue of the yeast Mcm3 replication protein. Nucleic Acids Res 20: 1069-1074.
- Valentine AM, Ishmael FT, Shier VK, Benkovic SJ (2001) A zinc ribbon

protein in DNA replication: primer synthesis and macromolecular interactions by the bacteriophage T4 primase. Biochemistry 40: 15074-15085.

- van Deursen F, Sengupta S, De Piccoli G, Sanchez-Diaz A, Labib K (2012) Mcm10 associates with the loaded DNA helicase at replication origins and defines a novel step in its activation. EMBO J 31: 2195-2206.
- Wang G, Klein MG, Tokonzaba E, Zhang Y, Holden LG, et al. (2008) The structure of a DnaB-family replicative helicase and its interactions with primase. Nat Struct Mol Biol 15: 94-100.
- Weisshart K, Forster H, Kremmer E, Schlott B, Grosse F, et al. (2000) Protein-protein interactions of the primase subunits p58 and p48 with simian virus 40 T antigen are required for efficient primer synthesis in a cell-free system. J Biol Chem 275: 17328-17337.
- Yang J, Xi J, Zhuang Z, Benkovic SJ (2005) The oligomeric T4 primase is the functional form during replication. J Biol Chem 280: 25416-25423.
- You Z, Komamura Y, Ishimi Y (1999) Biochemical analysis of the intrinsic Mcm4-Mcm6-mcm7 DNA helicase activity. Mol Cell Biol 19: 8003-8015.
- You Z, Ishimi Y, Mizuno T, Sugasawa K, Hanaoka F, et al. (2003) Thymine-rich single-stranded DNA activates Mcm4/6/7 helicase on Y-fork and bubble-like substrates. Embo J 22: 6148-6160.
- You Z, Masai H (2008) Cdt1 forms a complex with the minichromosome maintenance protein (MCM) and activates its helicase activity. J Biol Chem 283: 24469-24477.
- Zhu W, Ukomadu C, Jha S, Senga T, Dhar SK, et al. (2007) Mcm10 and And-1/CTF4 recruit DNA polymerase alpha to chromatin for initiation of DNA replication. Genes Dev 21: 2288-2299.

Chapter 3

The physical interaction of
Mcm10 with Cdc45
modulates their DNA binding properties

Introduction

3.1. INTRODUCTION

In eukaryotic systems, replication initiation is characterized by a multi-step sequential loading of many proteins onto the DNA. The eukaryotic DNA replication protein Mcm10 associates with chromatin in early S-phase and is required for assembly and function of the replication fork protein machinery. Another essential component of the eukaryotic replication fork is Cdc45, which is required for both initiation and elongation of DNA replication. One key component of the DNA replication machinery is the pre-replication complex (pre-RC), which assembles onto replication origins in late M/early G1 phases of the cell cycle, prior to the initiation of DNA replication at the beginning of S phase. The pre-RC consists of many proteins including Orc1–6, Cdc6 and Cdt1, whose binding to chromatin is a prerequisite for the recruitment of the helicase MCM2–7 [Lei M, Tye BK. (2001), Bell SP & Dutta A. (2002)]. At the G1-S transition, specific kinases (cyclin-dependent kinase, CDK and Dbf4-dependent kinase, DDK) phosphorylate components of the pre-RC promoting the unwinding of DNA and the recruitment of other important replication, such as the *m*ini-*c*hromosome *m*aintenance protein 10 (Mcm10), cell division cycle (Cdc) 45, and the GINS and Mcm2-7 complexes. One of the first proteins loaded onto chromosomal replication origins is the conserved factor Mcm10 [Wohlschlegel JA et al. (2002), Gregan J et al. (2003)]. Mcm10 does not have enzymatic activity rather studies performed on *Xenopus laevis* extracts showed that it binds to the pre-RC (one bound per 5000 bps, which means two per active origin). Physical interactions were observed between Mcm10 and many other replication factors, including the *o*rigin *r*ecognition *c*omplex (ORC) [Hart EA et al. (2002), Izumi M et al. (2000)], Mcm2-7, DNA polymerase (pol) α [Chattopadhyay & S, Bielinsky AK. (2007)], the helicase RecQ4 and acidic nucleoplasmic DNA-binding protein-1 (And-1) [Xu X et al. (2009), Zhu W et al. (2007)]. Mutations in Mcm10 cause a decrease in initiation of replication, but also a slow progression of DNA synthesis and stalling of replication forks during elongation [Merchant AM et al. 1997]. Recently, it was demonstrated that Mcm10 recruitment to the origin is eliminated by depletion of either Cdc45 or GINS [Heller RC et al.(2011)], suggesting that

those two proteins play a key role in the association of Mcm10 with the origin. Moreover, other lines of evidence suggest that chromatin-bound Mcm2–7 might also be involved in the recruitment of Mcm10 presumably via protein-protein interactions [Ricke RM & Bielinsky AK (2004)]. Interestingly, Cdc45 and RPA cannot load onto chromatin in Mcm10-depleted *Xenopus* egg extracts, preventing DNA unwinding and suggesting that Mcm10 may be a key component of the initiation machinery responsible for the melting of origin DNA sequence [Wohlschlegel JA et al. (2002)]. On the other hand, a recent report suggested that in *S. cerevisiae* Cdc45, Dpb11 and GINS are able to associate with the origin DNA even in the absence of Mcm10 [Heller RC et al. (2011)]. It has also been demonstrated that in *S. cerevisiae*, upon initiation of DNA replication, ScMcm10 moves from the origin to origin-proximal sequences, [Ricke RM & Bielinsky AK (2006)],. and several lines of evidence show that Mcm10 interacts with DNA pol α and DNA [Chattopadhyay & S, Bielinsky AK. (2007), Ricke RM & Bielinsky AK (2004), Warren EM et al. (2009)], suggesting that it associates with moving replication forks. Thus, the exact role(s) of Mcm10 in the initiation of DNA replication is not completely clear.

Limited proteolysis and mass spectrometry analyses revealed that *Xenopus* (X) Mcm10 is composed of three distinct structured domains at the N-terminal (NTD, residues 1-145), internal (ID, 230-427) and C-terminal (CTD, 596-860) regions of the protein [Robertson PD et al. (2008), Robertson PD et al. (2010)]. These three domains are tethered by linkers that are predicted to be largely unstructured and disordered. The NTD is a coil-coil domain that is believed to facilitate protein oligomerization. The ID is the most conserved region across all eukaryotes from vertebrate to yeast. It contains a CCCH-type zinc finger and an oligonucleotides/oligosaccharide binding (OB)-fold that facilitates its interactions with a number of proteins and with DNA [Izumi M et al. (2000), Ricke RM & Bielinsky AK (2006)]. In particular, it has been shown that xMcm10-ID can interact with single-stranded DNA and the N-terminal 323 residues of DNA pol α [Warren EM et al. (2009)]. The CTD is unique to higher eukaryotes; interactions between xMcm10-CTD and both DNA and DNA pol α have been observed [Warren EM et al. (2009), Robertson PD et al. (2008)]. The region involved in

this interaction is a proteolytically stable sub-domain that consists of a putative winged helix motif followed by tandem CCCH- and CCCC-type zinc motifs. It has been demonstrated [Okorokov AL et al. (2007)] that in solution human Mcm10 forms hexameric ring structures similarly to many other ring-shaped oligomeric DNA-binding proteins, such as the helicase complex Mcm2-7; however, human Mcm10 has no helicase motifs within its sequence and no detectable DNA helicase activity *in vitro*. Its ring structure may provide a structural basis for Mcm10 interaction with essential replication factors simultaneously.

Herein we present the first evidence of a direct interaction of human Mcm10 with Cdc45 (both *in vivo* and *in vitro*) and a stimulatory effect of Mcm10 C-terminal and Internal Domains (CTD and ID, respectively) on Cdc45 DNA binding activity. In addition, we present a detailed characterization of purified Mcm10 domains analyzing their oligomeric states and DNA binding activities.

Results

3.2. RESULTS

3.2.1. MCM10 AND CDC45 INTERACT IN HUMAN CELLS

Co-immunoprecipitation experiments with whole cell extracts and Cdc45 specific antibodies from asynchronous HEK293T cells were done to analyze the possible interaction between human Mcm10 and Cdc45. We found that Mcm10 was co-immunoprecipitated with Cdc45 (Fig. 1 lane 5). A negative control was performed incubating the resin with pre-immune serum as indicated in *Material and methods* (Fig. 1 lane 4). These results indicate that the two proteins interact in physiological conditions.

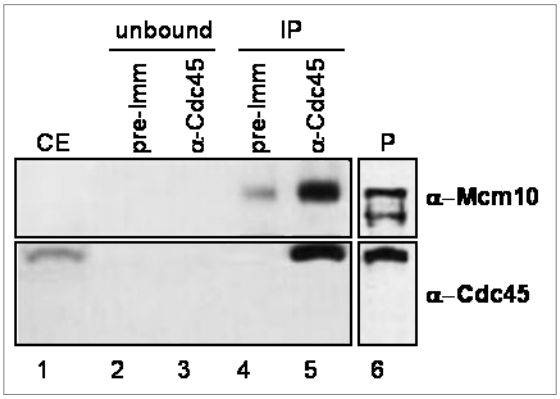

Figure 1. Mcm10 and Cdc45 interact in human cells. Whole cell lysates from HEK293T cells was immunoprecipitated with anti-Cdc45 or pre-immune serum as indicated. 30 mg of cell extract (CE, lane 1) of HEK293T were loaded. 10 mg of *E. coli* cell extract expressing human full-length Mcm10 were loaded together with 200 ng of purified human Cdc45 as control (P, lane 6). Antibodies against Mcm10 and Cdc45 were used for Western blotting analysis.

3.2.2. EXPRESSION AND PURIFICATION OF THE MCM10 ISOLATED DOMAINS

Next, we sought to map the interaction site of Mcm10 with Cdc45 and to study the functional consequences of their interaction *in vitro*. In order to do so, we attempted the purification of both proteins in their recombinant form. Attempts to produce full-length Mcm10 using either bacterial or baculovirus/insect cells

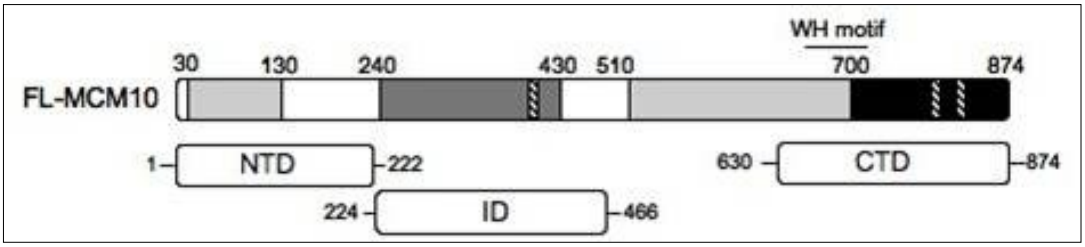

Figure 2. Analysis of human Mcm10 domains. Schematic representation of full length Mcm10 and its isolated domains, N-terminal, C-terminal and Internal Domains (NTD, CTD and ID, respectively) are shown. Light and dark grey bars indicate region of moderate and high sequence conservation, respectively, and hatched boxes represent invariant cysteine/histidine clusters involved in zinc coordination.

system led to low yield of recombinant protein that was highly unstable and/or insoluble. So we opted to study the fragments of human Mcm10 corresponding to the three structured domains previously identified in the *Xenopus* counterpart: NTD (1 to 222 amino acid, aa, residue), ID (224 to 466 aa residue) and CTD (630 to 874 aa residue) as shown in Fig. 2.

The open reading frames coding for CTD and ID were individually expressed in *E. coli* as hexa-Histidine-tagged proteins and purified to the homogeneity as described under *Material and Methods* (Fig. 3).

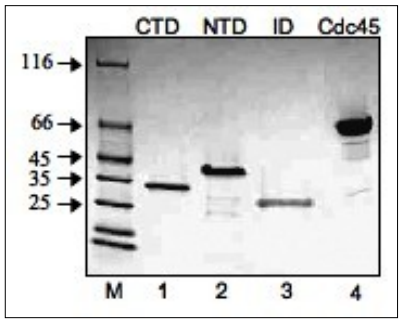

Figure 3. Purified recombinant proteins were run on a 10% SDS-PAGE gel that was stained with Comassie Blue. An aliquot of 20 µl of CTD (1 mg), NTD (2 mg), ID (0.5 mg) and Cdc45 (4 mg) were loaded (*lanes 1, 2, 3 and 4*, respectively); *M*, molecular weight markers (Fermentas).

To assess the oligomeric state of the Mcm10 truncated forms, we carried out gel filtration experiments using a Bio-Sil Sec-250 column (Bio-Rad). An apparent molecular mass of about 33 and 11 kDa was calculated for the purified recombinant CTD and ID, respectively (Fig 4B and 4D).

Considering that the minimal molecular weight of CTD and ID calculated on the basis of their aminoacidic sequence is about 27 kDa for both proteins, these results suggest that they predominantly form monomers in solution. The anomalous chromatographic behavior of ID could be due to its globular shape. The functionality of the CTD and ID domains was tested in DNA binding assays (EMSA). As shown in Fig. 4C and 4E, both domains were able to bind DNA (see also below), indicating a correct folding. The oligomeric state of the recombinant proteins was also investigated by glycerol gradient ultracentrifugation experiments that confirmed the results of the gel filtration analyses (data not shown).

Contrary to CTD and ID, the NTD (24 kDa) turned out to form hexamers in solution showing a molecular weight of 107 kDa (Fig. 4A). This result is in agreement with the observation by Okorokov *et al.* that human Mcm10 forms

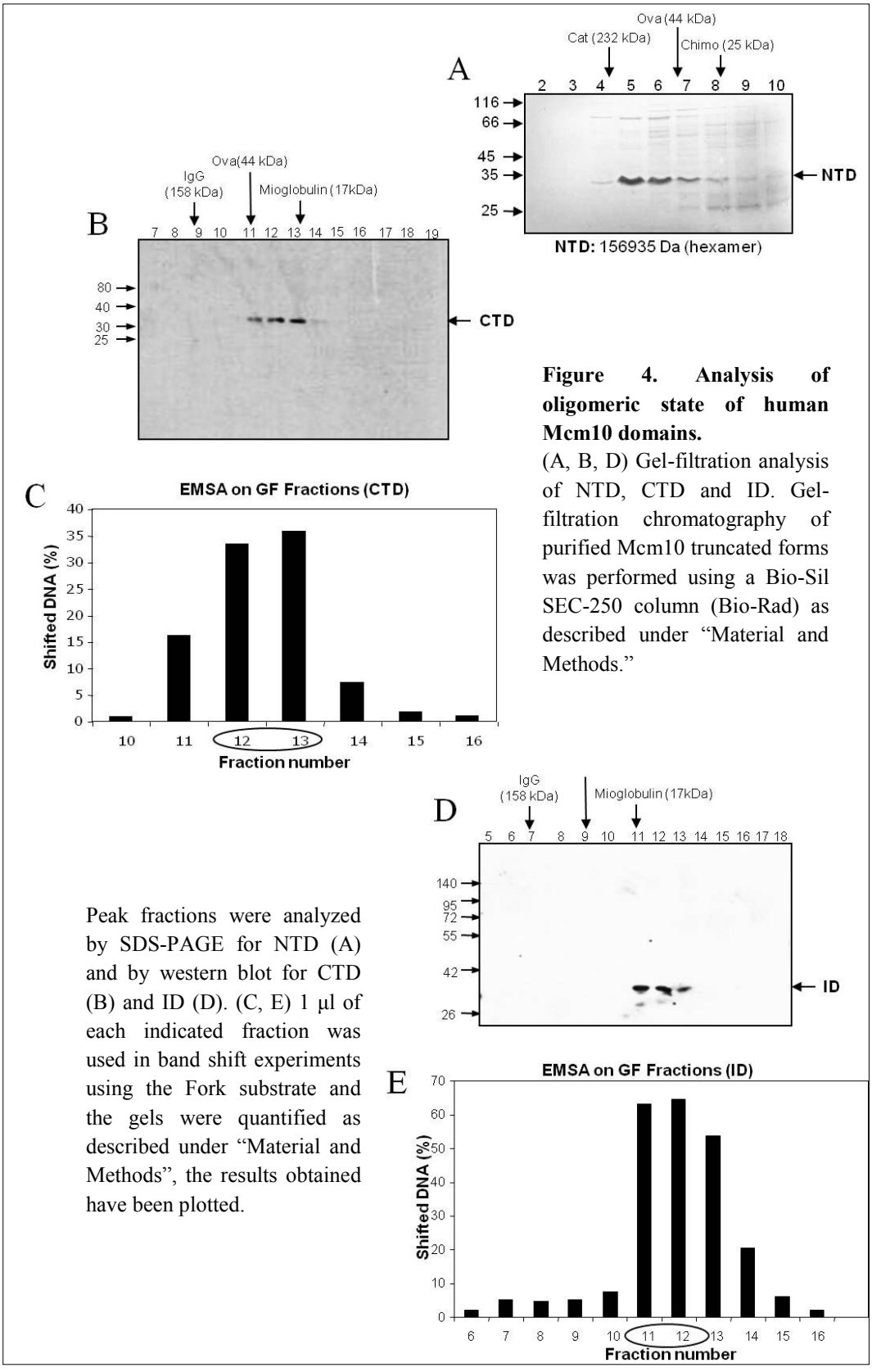

Figure 4. Analysis of oligomeric state of human Mcm10 domains.

(A, B, D) Gel-filtration analysis of NTD, CTD and ID. Gel-filtration chromatography of purified Mcm10 truncated forms was performed using a Bio-Sil SEC-250 column (Bio-Rad) as described under "Material and Methods."

Peak fractions were analyzed by SDS-PAGE for NTD (A) and by western blot for CTD (B) and ID (D). (C, E) 1 µl of each indicated fraction was used in band shift experiments using the Fork substrate and the gels were quantified as described under "Material and Methods", the results obtained have been plotted.

hexamers and that the N-terminal region is responsible for the oligomerization of the protein [Okorokov AL et al. (2007)].

It has been proposed by Robertson *et al*. that also *Xenopus* Mcm10 N-terminal domain is responsible for the oligomerization of the full-length protein; however, *Xenopus* recombinant Mcm10 NTD protein formed dimers in solution [Robertson PD et al (2008)].

3.2.3. PHYSICAL INTERACTION OF MCM10 DOMAINS WITH CDC45

The results of the IP experiments from human cells suggested a possibility that some domains of Mcm10 may interact with Cdc45 directly. To analyze the direct association between CTD and Cdc45 co-immunoprecipitation experiments were carried out using protein A agarose resin conjugated with antibodies against Cdc45. As shown in Fig.5, lane 4, Cdc45 was able to associate with CTD.

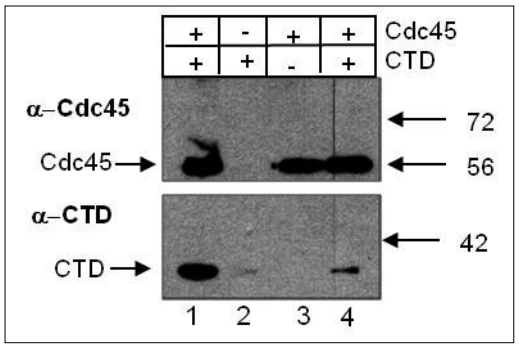

Figure 5. Physical interaction between Cdc45 and CTD. Immunoprecipitation experiments were carried out using protein A sepharose beads conjugated with anti-Cdc45 antibodies incubated with CTD. After the elecrophoretic run, the gel was transferred to a PVDF membrane which was cut into two halves: the upper part was analyzed using anti-Cdc45 antibodies while the lower half was analyzed using anti-CTD antibodies. The detection was performed using the ECL+ system. Lane 1 contains input 200 ng of recombinant purified Cdc45 and CTD.

In contrast, neither ID nor NTD were able to physically interact with Cdc45 under these experimental conditions (Fig. 6).

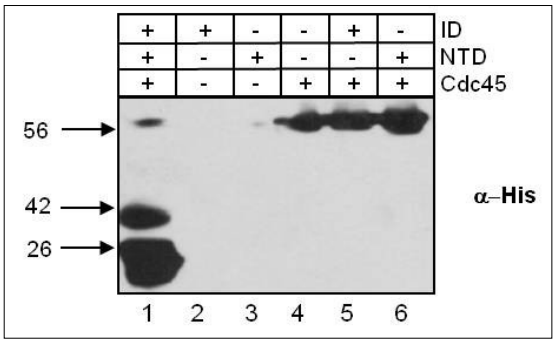

Figure 6. Physical interaction between Cdc45 and ID or NTD. Immunoprecipitation experiments were carried out using protein A sepharose beads conjugated with anti-Cdc45 antibodies incubated with ID or NTD. All the proteins analyzed contain a His-tag which was exploited for the detection. After the elecrophoretic run, the gel was transferred to a PVDF membrane and analyzed using anti-His antibodies and detected with the ECL+ system. Lane 1 contains input recombinant purified Cdc45, ID and NTD (200 ng).

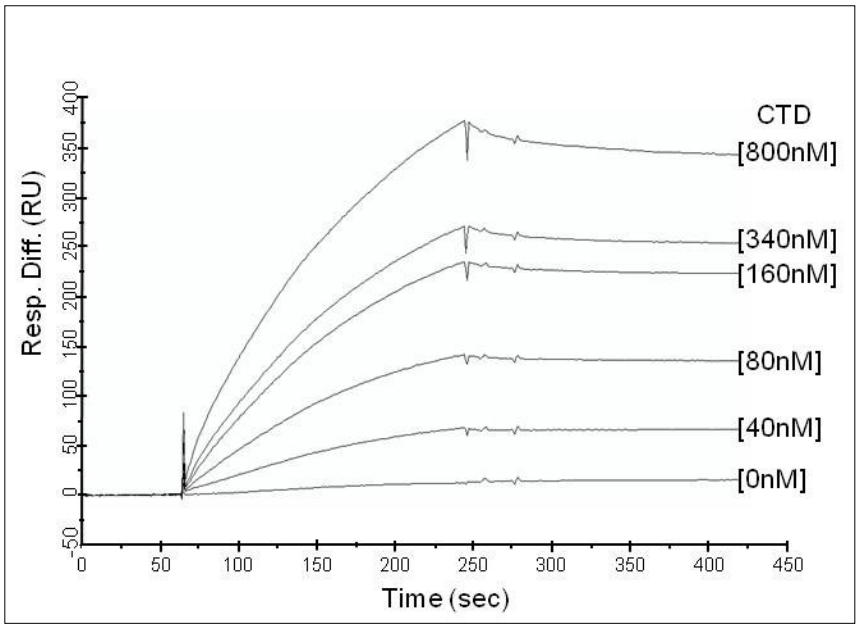

Figure 7. Physical interaction between Cdc45 and CTD. Physical interaction between CTD and Cdc45 analyzed by surface plasmon resonance. The plot shows sensorgrams obtained by fluxing protein at indicated concentrations over a Cdc45-immobilised sensor chip, as described in "Material and Methods".

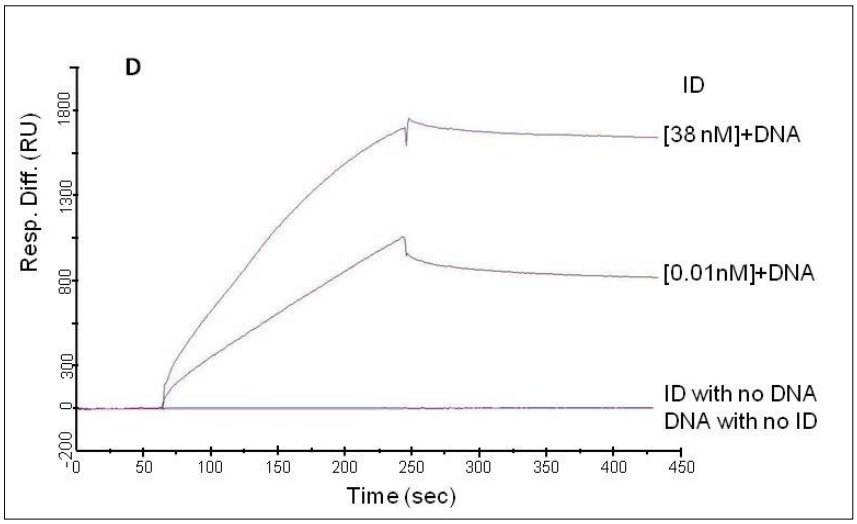

Figure 8. Physical interaction between Cdc45 and ID. Physical interaction between ID and Cdc45 analyzed by surface plasmon resonance. . The plot shows sensorgrams obtained by fluxing protein at indicated concentrations over a Cdc45-immobilised sensor chip, as described in "Material and Methods". The two indicated amounts of ID were previously incubated with 1 pmol of bubble shaped DNA, then fluxed over the same sensor chip used for CTD measurements. ID and DNA were fluxed separately as negative controls.

The physical association of Cdc45 with CTD was then confirmed by surface plasmon resonance measurements using a BIACORE 2000 instrument. In these experiments, increasing concentrations of CTD (from 0 to 800 nM) were passed over a Cdc45-immobilized CM5 sensor chip, as described under *Material and Methods*. Figure 7 shows typical overlaid sensorgrams obtained by testing increasing concentrations of protein. This analysis indicated that Cdc45 physically interacts with Mcm10 CTD and a quantitative analysis of the sensorgrams revealed a K_D of 1.02 $x10^{-8}$ M and a

K_A 9.79 $x10^{-7}$ M indicating that the two proteins interact stably.

Increasing amounts of ID were also fluxed over the Cdc45-immobilized sensor chip in the same conditions used for CTD (see *Material and Methods*), but no increasing curves were observed in this case. These results were unexpected, since we argued that also ID should interact with Cdc45 on the basis of the DNA band shift experiments. Therefore, we hypothesized that DNA could be necessary for the interaction of these two proteins and decided to pre-incubate Mcm10 ID with a fixed amount of bubble-containing DNA (1 pmol) before fluxing it over the sensor chip. Figure 8 shows the sensorgrams obtained in these conditions. When the DNA substrate or ID where fluxed alone over Cdc45-immobilized sensor chip, no signal was detected. On the contrary, a clear increase in the resonance was observed when both ID and DNA were present together, which increased as the ID concentration was raised. These results confirm our hypothesis that interaction of ID and Cdc45 takes place only in the presence of DNA.

3.2.4. DNA BINDING ACTIVITY OF THE MCM10 DOMAINS

The ability of CTD, ID and NTD to bind DNA was assayed using electrophoretic mobility shift assays with a variety of synthetic oligonucleotides: molecules containing a bubble of 20 T residues (Bub-20T), flayed duplexes with tails of 20 T residues (Fork), 3'- or 5'-tailed duplexes (3'-Tail and 5'-Tail), blunt DNA duplexes, and single-stranded DNA oligonucleotides (see Table 1).

Name	*Sequence*
dsDNA	Strand1: 5'- GCTCGGTACCCGGGGATCCTCTAGA -3' Strand2: 5'- TCTAGAGGATCCCCGGGTACCGAGC -3'
3'- mis	Strand1: 5'- CTTGCATGCCTGCAGGTCGACTCTAGAGGATCCCCGGGTAC CGAGC-3' Strand2: 5'- TCCTCTAGAGTCGACCTGCAGGCATGCAAG -3'
5'-mis	Strand1: come filamento 1 del 3'-mis Strand2: 5'-TCACACAGGAAACAGCTATGACCATGATTA -3'
Bubble	Strand1: 5'- GCTCGCTACCTCTACCTGGACGACCGGG$(T)_{20}$GGGCCAGCAG GTCCATCACCATCGCTCG- -3' Strand2: 5'-CGAGCGATGGTGATGGACCTGCTGGCCC $(T)_{20}$CCCGGTCGTCCAGGTAGAGGTAGCGAGC -3'
Fork	Strand1: 5'- GCTCGGTACCCGGGGATCCTCTAGATTTTTTTTTTTTTTTTT TT -3' Strand2: 5'- TTTTTTTTTTTTTTTTTTTTTCTAGAGGATCCCCGGGTACCGAG C -3'
ssDNA 25mer	Strand: 5'- GCTCGGTACCCGGGGATCCTCTAGA-3'
ssDNA 56mer	Strand: 5'-TCTACCTGGACGACCGGGTATATAGGGC CCTATATATAGGGCCAGCAGGTCCATCA- 3'

Table 1. Oligonucleotides used for DNA substrates preparation

Both CTD and ID preferentially bound to the Bub-20T, Fork and 3'-Tail or 5'-Tail DNA molecules with respect to Blunt or ss DNA, as evident from the dose-dependent formation of the shifted bands, as shown in Fig. 9 (CTD) and Fig. 10 (ID).

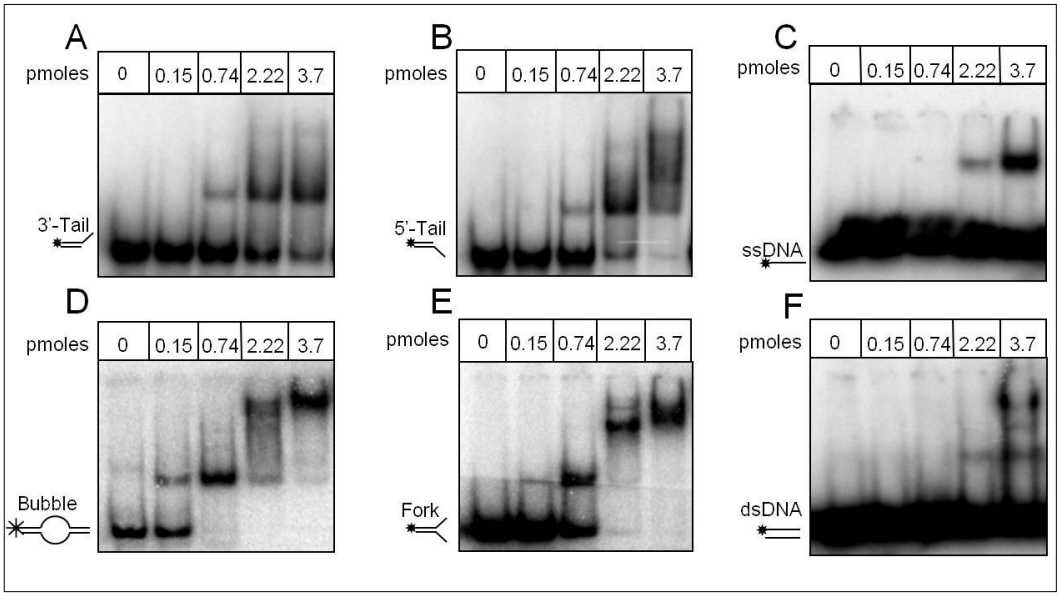

Fig.9. DNA binding activity of CTD on various DNA molecules. DNA band shift assays were carried out on the DNA molecules schematically indicated on the left of each gel using increasing amounts of CTD as described under "Material and Methods". The *lanes* marked with 0 were loaded with control samples without protein.

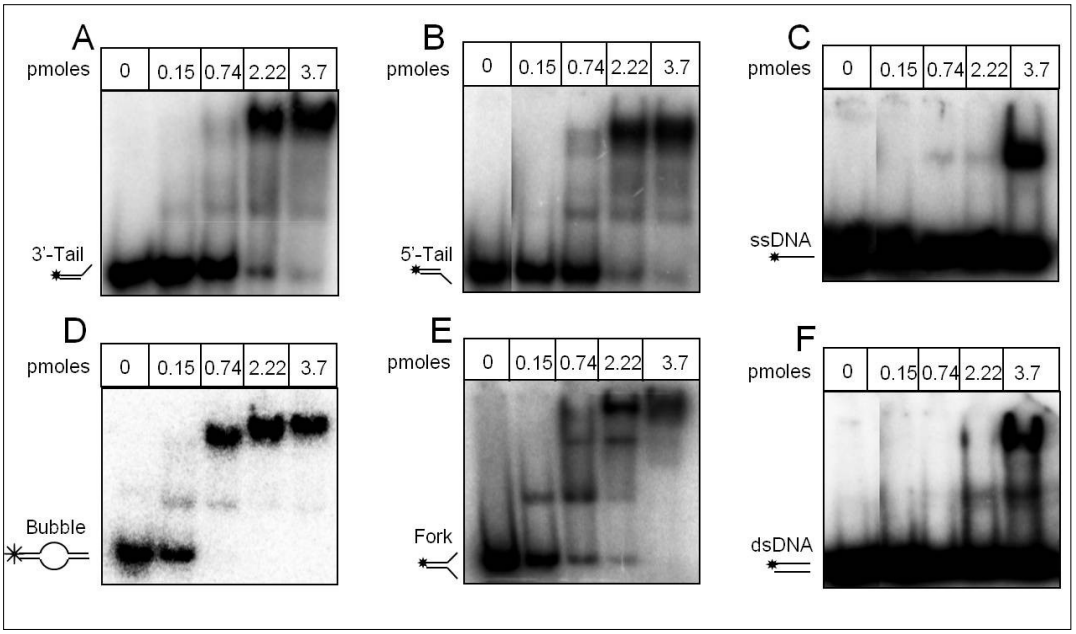

Figure 10. DNA binding activity of ID on various DNA molecules. DNA band shift assays were carried out on the DNA molecules schematically indicated on the left of each gel using increasing amounts of ID as described under "Material and Methods". The *lanes* marked with 0 were loaded with control samples without protein.

A quantitative analysis of these experiments confirmed the clear preference of both ID and CTD for bubble- and fork-containing ligands. On the other hand, single-stranded oligonucleotides or blunt duplexes were bound with about 5 to10 fold less efficiency in comparison to fork and bubble ligands (Fig. 11, A and B, Table 2).

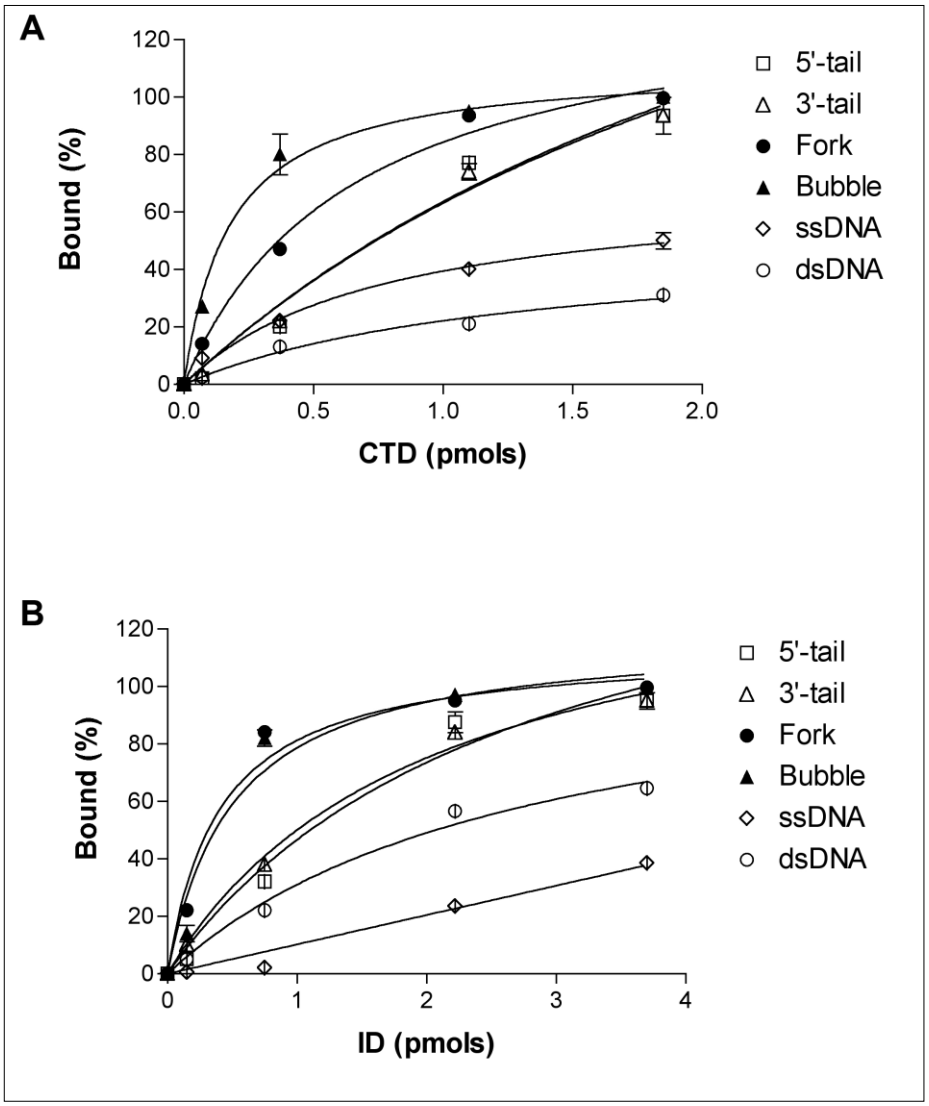

Figure 11. Analysis of the shifted DNA *versus* the amount of protein used. Increasing amounts of CTD or ID were used in the presence of various DNA structures, panel A and B, respectively. The percentage of shifted DNA was plotted against the amount of protein used in each assay. Symbols used are: *open circles* (double-stranded DNA), closed circles (fork), *open squares* (5′Tail), closed triangles (bubble), open triangles (3′Tail), diamonds (single-stranded DNA).

Substrate	CTD	CTD+Cdc45	ID	ID+Cdc45	Cdc45	Cdc45+ID	Cdc45+CTD
	Kd (μM)	*Kd* (μM)	*Kd* (μM)	*Kd* (μM)	*Kd* (μM)	*Kd* (μM)	*Kd* (μM)
5'-tail	0.302±0.009		0.27±0.05				
3'-tail	0.296±0.005		0.2±0.01				
Fork	0.075±0.003		0.04±0.006				
Bubble	0.037±0.01	0.01±0.003	0.05±0.01	0.005±0.001	8.1±0.05	0.3±0.01	0.4±0.03
ssDNA	0.1±0.02		0.2±0.02				
dsDNA	0.13±0.01		1.5±0.5				

Table 2. DNA binding kinetic parameters referred to the indicated proteins

In particular, CTD showed a K_D of 0.037 μM and 0.075 μM for DNA with bubble and fork, respectively, whereas ID binds the same molecules with K_D values of 0.05 μM and 0.04 μM, respectively. The main difference between CTD and ID is that ID shows a weaker (o less efficient) binding to dsDNA. In fact, as shown in Table 2, ID and CTD possess a K_D of 1.5 μM and 0.13 μM, respectively, for the binding to this substrate. This preference for DNA substrates mimicking replication intermediates is in line with the proposal that Mcm10 plays a role both in initiation and elongation phases of DNA replication.

We also tested the ability of CTD and ID to bind oligo-dC, oligo-dG, oligo-dT and oligo-dA molecules, but we observed no retarded DNA bands for all of these synthetic oligonucleotides (data not shown).

When a similar analysis was performed with NTD, we observed no binding to any of the DNA molecules tested (data not shown).

Taken together, these data indicate that CTD and ID are responsible for the DNA binding activity of human Mcm10.

As mentioned above, we analyzed the DNA binding activity of the protein fractions following analytical size-exclusion chromatography. We found that DNA-binding activity profile precisely corresponded to the ID and CTD protein peak (Fig. 4C and 4E) suggesting that the ability to bind DNA is a intrinsic feature of the two Mcm10 truncated forms and is not due to trace amounts of a contaminating protein.

3.2.5. MCM10 ID COOPERATES WITH CDC45 IN BINDING DNA

We decided to analyze the mutual effect of NTD, CTD or ID in combination with Cdc45 on the binding to oligonucleotides containing a bubble structure. When ID (from 0.03 to 0.3 pmol) was titrated alone with the Bub-20T DNA, it produced a main retarded band in electrophoretic mobility shift assays (Fig. 12A, lanes 3 to 6). On the other hand, Cdc45 (about 37 pmol) incubated alone with the same DNA substrate also formed a retarded band, but its binding was less efficient than ID (Fig. 12A, compare lane 2 with lane 6).

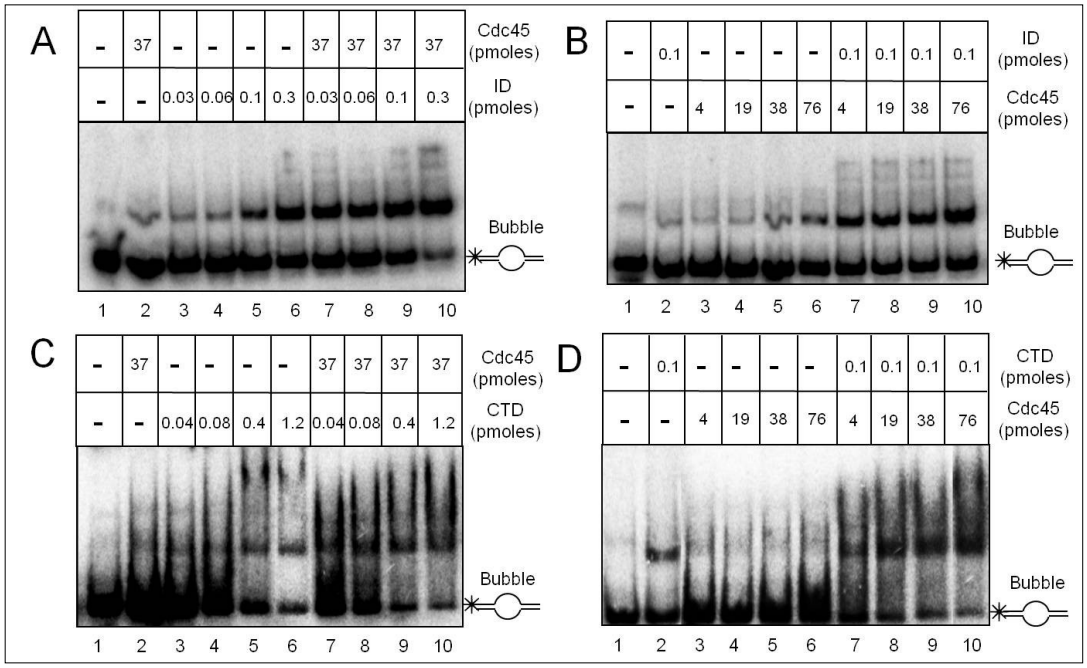

Figure 12. Effect of ID and CTD on Cdc45 DNA binding activity. *Panel A*, DNA band shift assays were carried out on the bubble-containing DNA molecules using increasing amounts of ID (from 0.03 to 0.3 pmoles as indicated on the top of the gel) in the absence (lanes 3–6) or in the presence (lanes 7–10) of Cdc45 (37 pmoles). *Panel B,* increasing amounts of Cdc45 (from 4 to 76 pmoles as indicated on the top of the gel) were incubated in the absence (lanes 3–6) or in the presence (lanes 7–10) of a fixed amount of ID (0.1 pmoles). *Panel C*, increasing amounts of CTD (from 0.04 to 1.2 pmoles as indicated on the top of the gel) in the absence (lanes 3–6) or in the presence (lanes 7–10) of Cdc45 (37 pmoles). *Panel D,* increasing amounts of Cdc45 (from 4 to 76 pmoles as indicated on the top of the gel) were incubated in the absence (lanes 3–6) or in the presence (lanes 7–10) of a fixed amount of CTD (0.1 pmoles).

When ID and Cdc45 were mixed together in the above experimental conditions, complex formation was increased with respect to the condition in which the two proteins were incubated separately with the DNA ligand, and this increase was proportional to the concentration of ID used (Fig. 12A, lanes 7 to 10).

In a subsequent set of experiments, the amount of ID was kept constant at a value that produced only a minimal signal of the retarded band (0.1 pmol, see Fig. 12 B, lane 2), whereas the amount of Cdc45 was increased from 4 to 76 pmol, a range of values that produced a visible DNA band shift (Fig. 12*B*, lanes 3 to 6). Again, when ID and Cdc45 were mixed together, the amount of complex formed was significantly increased (Fig. 12*B*, lanes 7 to 10). These results indicate that Cdc45 and ID cooperate for the binding to bubble-containing oligonucleotides. A similar effect was also observed when fork-containing and single-stranded DNA molecules were used as ligands in the band shift assays, although to a lesser extent (data not shown).

The same experiments were conducted mixing CTD and Cdc45. First we used a fixed amount of Cdc45, which gave a faint retarded band (Fig. 12C lane 2), and, separately, increasing amounts of CTD (Fig. 12C, lanes 3 to 6). When the two proteins were mixed together (Fig. 12C, lanes 7 to 10) in the above experimental conditions, we observed a clear increase of the shifted DNA band and a gradual reduction of the free probe DNA. Afterwards the amount of CTD was kept constant while Cdc45 was increased from 4 to 76 pmol (Fig 12D, lanes 2 and 3 to 6, respectively): the amount of free probe DNA was drastically reduced and the retarded bands were more abundant already at the first amount of CTD used (Fig. 12D, lanes 7 to 10). Furthermore, this effect (for both CTD and ID) was not dependent on the order of addition of the two proteins into the mixtures containing the DNA molecules (data not shown).

A similar effect was not observed in control experiments where, instead of CTD or ID, we used equal amounts of various unrelated proteins (data not shown).

3.2.6. MCM10 CTD, BUT NOT NTD, COOPERATES WITH CDC45 IN BINDING DNA

The same set of experiments was also carried out using the NTD fragment, but no stimulatory effect on Cdc45 binding activity was observed in all conditions tested (data not shown). Overall, these data indicate that the stimulation of Cdc45 DNA binding activity is a specific effect of Mcm10 CTD and ID.

Quantification of the band shift experiments (Fig. 13A and B) allowed the determination of the kinetic parameters reported in Table 2.

A clear stimulation of the DNA binding function of Cdc45 in the presence of Mcm10 truncated forms was observed. In fact, when Cdc45 was mixed with either CTD or ID, the binding affinity of Cdc45 for bubble DNA was increased of about 20 folds. Reciprocally, in the presence of Cdc45, the affinity of ID for the bubble showed a 10-fold increase, while that of CTD raised of about 4-fold. In conclusion, the complex made by Cdc45/CTD or Cdc45/ID binds the bubble structure better than the corresponding proteins on their own. However, since the most evident stimulatory effect was on Cdc45, we can assume that is it Mcm10 domains CTD and ID that stimulate Cdc45 DNA-binding more than the reciprocal.

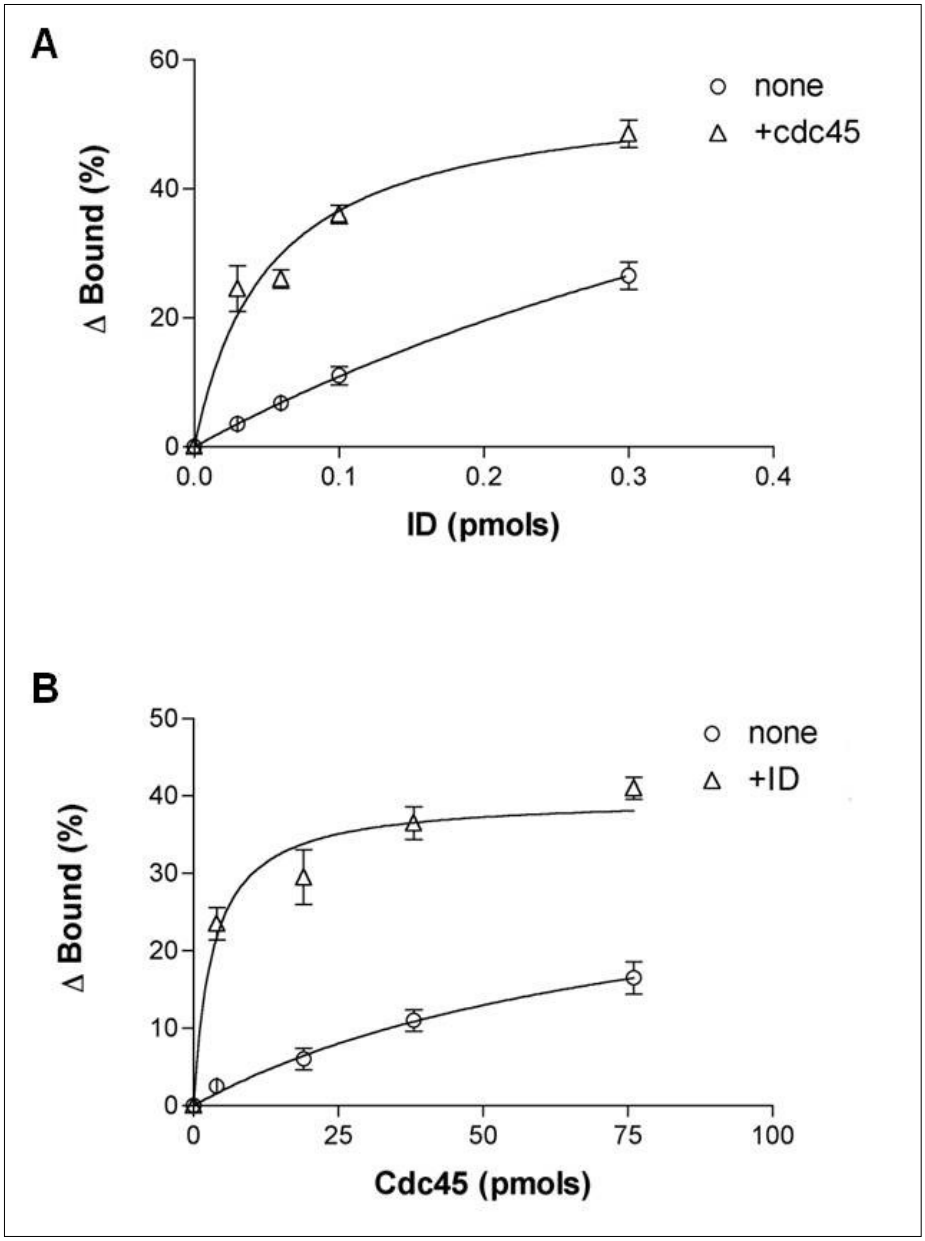

Figure 13. Analysis of the shifted DNA *versus* the amount of protein used. Panel A. Increasing amounts of ID were used in the absence (open circles) or presence (open triangles) of a fixed amount of Cdc45. The % of shifted DNA was plotted against the amount of protein used. Panel B. Increasing amounts of Cdc45 were used in the absence (open circles) or presence (open triangles) of a fixed amount of ID using the bubble DNA substrate.

Discussion

3.3. DISCUSSION

Studies performed on *Xenopus* extracts showed that Mcm10 is necessary for the loading of Cdc45, which in turn is essential for chromatin unwinding at the origin [Wohlschlegel JA et al (2002)]; however, no direct interaction of Mcm10 and Cdc45 has been observed so far. Here, we show, by co-immunoprecipitation experiments with whole human cell extracts, a specific interaction between Mcm10 and Cdc45 in physiological conditions. Starting from these data we decided to analyze the details of the direct interaction between human Cdc45 and Mcm10. Previous biochemical and structural studies suggested that Mcm10 can be divided into three structured domains; however, the relative contributions of these domains to the biochemical properties of Mcm10 are still poorly characterized. We thus decided to perform a biochemical study of the human Mcm10 domains. Biochemical and structural analyses have been controversial with regard to the oligomeric state of the full-length Mcm10 protein: several studies identify *Xenopus* Mcm10 assemblies composed of two or three subunits [Robertson PD et al. (2008)], whereas human Mcm10 was reported to form a ring-shaped hexameric structure [Okorokov AL et al. (2007)]. The ring-like architecture of Mcm10 suggests that this replication protein might have conserved the ability to encircle DNA similarly to other proteins involved in DNA metabolism [Eisenberg S et al. (2009), Hingorani MM & O'Donnell M. (1998)], thus forming a topological link and a structural scaffold between replication factors and the nucleic acid. We have performed gel filtration and glycerol gradient analysis in order to establish the oligomeric state of human Mcm10 NTD, ID and CTD. Our data showed that NTD forms hexamers in solution, in agreement with what was previously reported [Okorokov AL et al. (2007)]. On the contrary, the two other Mcm10 domains formed monomers. The results obtained for NTD suggest that this region could be responsible for the oligomerization of Mcm10, in agreement with the proposal of Robertson et al. [Robertson PD et al. (2008)] that revealed the presence of a coiled-coil domain at the N-terminus of the protein. Moreover, the hypothesis that NTD might function as an oligomerization domain for the full-length Mcm10 was recently reinforced

by Apger *et al.* [Apger J et al. (1010)] on the basis of a strong one-hybrid interaction from the first 100 residues of *Drosophila* homolog. Interestingly, self-interaction of ID and CTD was also observed in yeast 2-hybrid assays when the NTD was deleted, indicating that the NTD may not be the only point of contact between Mcm10 subunits [Robertson PD et al. (2008)].

We then investigated a possible direct interaction between Cdc45 and each domain of Mcm10 by both co-immunoprecipitation experiments and surface plasmon resonance analyses. The recombinant form of human Cdc45 was previously produced in our laboratory and we have demonstrated that it is able to bind single-stranded, but not double-stranded DNA [Krastanova I et al. (2012)]. These experiments confirmed the interaction of Mcm10 and Cdc45 and in particular we observed that CTD is able to directly interact with Cdc45 while NTD is not. Interestingly, ID interacts with Cdc45 only when pre-incubated with DNA, suggesting that ID undergoes DNA-induced conformational changes that may allow it to interact with Cdc45.

Previous studies performed in other systems showed that Mcm10 binds DNA. Fien and Hurwitz [Fien K & Hurwitz J. (2006)] reported that SpMcm10 binds well to ssDNA but barely interacts (20-fold lower affinity) with dsDNA. Eisenberg et al. [Eisenberg S et al. (2009)] analyzed ScMcm10 DNA binding activity demonstrating that it is able to bind both single and double-stranded DNA. This behavior can be important for Mcm10 functions in initiation, establishment of replication forks and maintenance of replisome progression during chromosomal DNA replication. Recently, it was reported that a DNA binding activity is also associated with full-length xMcm10 and its truncated forms. These studies showed that the affinity of each domain for single-stranded DNA was about 2-fold greater than for double-stranded DNA, whereas the full-length protein bound all tested DNA ligands with the same affinity. Our results clearly showed that CTD and ID preferred DNA structures that mimic the replication origin (bubble) and the elongating DNA (fork). On the basis of these results we suggest that Mcm10 is anchored to DNA throughout replisome assembly. As expected, NTD does not bind DNA, in agreement with what previously observed by Robertson et al [Robertson PD et al. (2008)] for xMcm10.

The differences in structure and DNA binding may reflect differences in the function of Mcm10 in various organisms as well as in the protein preparations.

Finally, we decided to analyze if there was a mutual effect on DNA binding of the two proteins. We first analyzed the effect of each truncated form on Cdc45 binding to DNA and *vice-versa*. Interestingly, we observed a mutual stimulation of DNA binding by both CTD and ID and Cdc45, while NTD did not have any effect. K_D values suggest that Cdc45 is stimulated by CTD and ID more then the reciprocal.

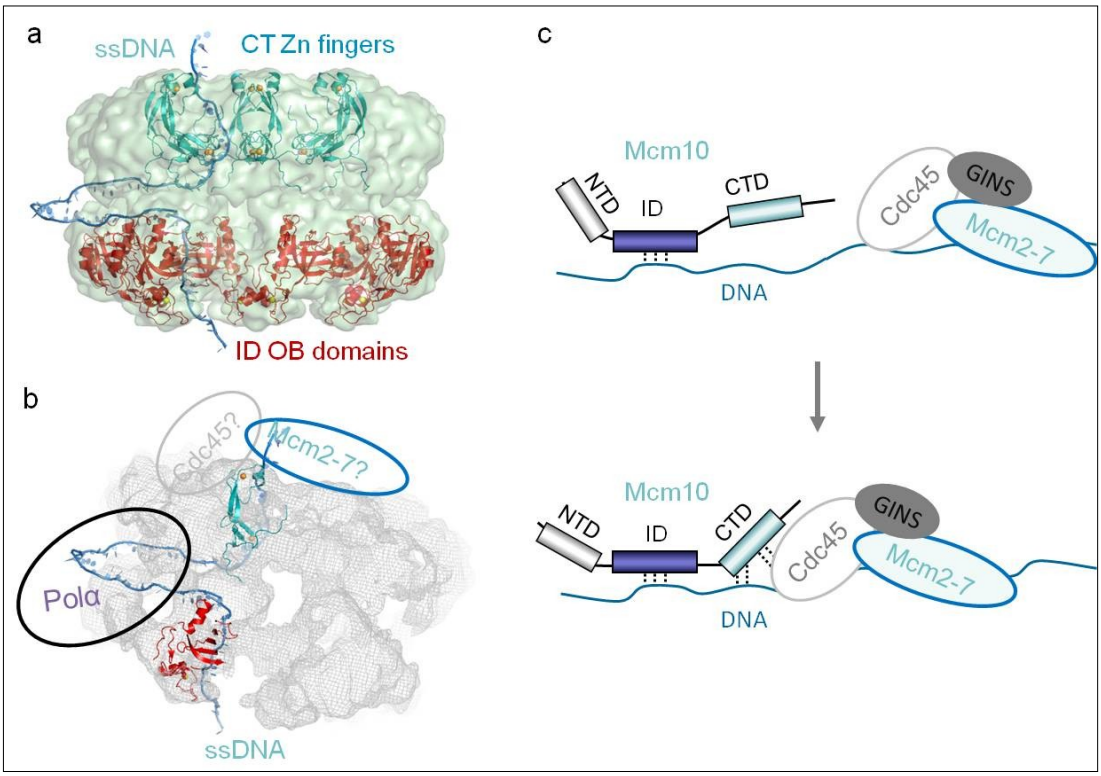

Fig. 14. Mcm10 domains and Cdc45 interaction. (a) Mcm10 domain structures were fitted into the Mcm10 3D EM map. ID (in red) and CTD (in cyan) shown as cartoons. Zn atoms are show as orange (for CTD) and yellow (for ID) spheres. ssDNA fit model is shown in blue tracking through the Mcm10 ring with one end bound to ID, then protruding into the opening on a side of the molecule, forming a loop and entering back to bind CTD. (**b**) Same as for 9a) with indicated areas of DNA Pol α, Cdc45 and Mcm2-7 interaction.
(**c**) Schematic representation of Mcm10 recruitment to CMG on DNA. Mcm10 bound to DNA via ID encounters CMG and is anchored to it via additional contacts to DNA and Cdc45 facilitated via CTD.

Modular architecture is a common feature of DNA processing proteins that allows for the coordination of distinct biochemical activities [Stauffer ME & Chazin WJ. (2004)]. The structural organization of Mcm10, which is made by structured domains connected by flexible linkers, allows Mcm10 domains to accommodate DNA and proteins simultaneously.

According to our results we propose a model shown in Fig. 14, in which human Mcm10 domains (ID and CTD) were located by docking their known atomic structures, and the areas of DNA pol-α, PCNA, Mcm2-7 and Cdc45 contacts with Mcm10 are indicated according to existent biochemical data [Warren, E.M. & Eichman, B.F. (2008), and this paper]. A path of the single-strand DNA through the Mcm10 ring is hypothetic, and is based on how it is envisaged for DNA helicase rings in other systems [Patel SS & Picha KM (2000)], and how OB-folded domains bind DNA in Mcm10 and other proteins [Robertson PD et al. (2010), Bochkarev A & Bochkareva E. (2004)]. The important difference between Mcm10 and DNA helicases though is that Mcm10 does not have any ATP-provided motor energy, so most likely that the motion of DNA is provided by Mcm2-7 pumping DNA through and possibly by the movement of the DNA template by DNA pol-α. Of special interest is the fact that unlike CTD, the ID domain of Mcm10 interacts with Cdc45 only in the presence of DNA. One can potentially envisage a putative mechanism that directs Mcm10-Cdc45-DNA interaction into a productive complex during replisome assembly (Fig. 14). For example, Mcm10 may bind any Cdc45 and/or replicative DNA helicase complex CMG (Cdc45/Mcm2-7/GINS) via CTD of Mcm10, but the interaction would only be complete and productive for initiation when Mcm10 is bound to DNA via its ID part. It follows then, that Mcm10 ID DNA-binding might be an initial step that brings Mcm10 close to CMG complex. When DNA-bound Mcm10 (via ID) encounters CMG it then may interact with Cdc45 via CTD thus stabilizing the overall complex and facilitating additional DNA-anchoring. Moreover, the overall Mcm10-CMG complex may be further stabilized by additional contacts between Mcm10 and Mcm2-7. Notably, the ID prefers ssDNA as a binding substrate, so the initial interaction is more likely to take place when CMG produces a stretch of ssDNA for initial DNA unwinding. This is in keeping with recent reports of

Mcm10 activating CMG-induced DNA unwinding (van Deursen F et al. (2012), Kanke M et al. (2012), Watase G et al. (2012)]. Another possibility is that Mcm10 may be initially recruited to DNA replication origins by interaction with Mcm2-7, as was reported in Wohlschlegel JA et al. [Wohlschlegel JA et al. (2002)] and this interaction helps to recruit Cdc45 and GINS, and stabilize contacts between all components of this complex. Our data now suggest that Mcm10-CMG complex interaction appears to be a part of a cooperative DNA-binding and activity stimulation event. It is plausible that Mcm10 stimulates CMG-induced unwinding of DNA and at the same time this initial unwinding stimulates Mcm10 binding to both ssDNA and CMG (via Cdc45) to form stable productive complex that forms a core part of replisome.

Materials

&

Methods

3.4. MATERIALS AND METHODS

3.4.1. PRODUCTION OF RECOMBINANT PROTEINS

Human Cdc45 was purified as described by Krastanova et al. [Krastanova I et al. (2012)]. *E. coli* Rosetta cells (Novagen) transformed with the plasmid pET15b-CTD, pProEX-NTD and pProEX-ID were grown separately at 37 °C in 1 liter of LB (Luria-Bertani) medium containing 30 μg/ml chloramphenicol and 100 μg/ml ampicillin. When the culture reached an A_{600} of 0.8, protein expression was induced by adding isopropyl β-D-thiogalactoside at a concentration of 1 mM. The bacterial culture for the production of MCM10-ID was incubated at 37 °C for an additional 2 hours, while those for expression of MCM10-NTD, MCM10-CTD and Mcm10-ID were incubated at 18 °C for an additional 12 hours. Cells were then harvested by centrifugation (10800 *g* for 10 min at 4 °C) and the pellet (5 g) was stored at -20 °C until use. The cell pellet was thawed and re-suspended in 20 ml of buffer A [20mM Tris/HCl (pH 7.5), 2.5 mM $MgCl_2$, 500mM NaCl, 3.5mM β-mercaptoethanol, 10 mM imidazole, 10% glycerol] supplemented with protease inhibitors cocktail (Roche), Cells were broken by two consecutive passages through a French pressure cell apparatus (Aminco Co) at 1500 p.s.i. The resulting cell extract was treated with DNase I (at 0.25 mg/ml) and RNase A (at 0.1 mg/ml) for 30 min on ice with shaking. Protamine sulfate (at 2 mg/ml) was then added and incubation was continued for an additional 30 min on ice with shaking. The sample was centrifuged for 30 min at 30000 rev/min (Beckman rotor 70.0 Ti) at 4 °C. The supernatant was passed through a 0.22 μm filter (Millipore), mixed with Ni^{2+}-nitrilotriacetic acid Superflow-agarose resin (Qiagen), pre- equilibrated in buffer A and incubated for 1 h on ice with gentle shaking. The resin was washed with buffer A and elution was carried out with 20 ml of an imidazole gradient (50-500 mM) in buffer A. Fractions of 0.5 ml were collected and analyzed by SDS-polyacrylamide gel electrophoresis (SDS/PAGE) to detect the Mcm10-CTD, Mcm10-NTD and Mcm10-ID. Fractions containing the recombinant proteins were pooled and dialyzed overnight against buffer A containing 150 mM NaCl. The sample containing Mcm10-CTD or Mcm10-NTD was loaded onto a Superdex 200 16/60 column (GE Healthcare Life Sciences) equilibrated in buffer A containing

150 mM NaCl. The column was developed at a flow rate of 0.5 ml/min. Fractions of 1 ml were collected and a sample of each of them (20 µl) was analyzed by SDS/PAGE. Fractions containing Mcm10-CTD or Mcm10-NTD were stored at -20 °C for subsequent biochemical analyses. The sample containing Mcm10-ID was loaded onto a heparin-Sepharose column (5 ml) at 0.5 ml/min using an AKTA system (GE Healthcare Life Sciences). The column was equilibrated and washed in the same buffer. The bound protein was eluted using a linear gradient of NaCl in buffer (from 0.15 to 1 M NaCl). Fractions containing Mcm10-ID were pooled and stored at -20 °C for subsequent biochemical analyses.

To analyze the oligomeric state of the truncated forms, samples of the recombinant proteins were loaded onto a Bio-Sil Sec-250 column (Bio-Rad) equilibrated in buffer A containing 150 mM NaCl. The column was developed at a flow rate of 0.3 ml/min. Fractions of 0.5 ml were collected and analyzed by SDS-PAGE. The column was calibrated by running a set of gel filtration markers that included tyroglobulin (669 kDa), IgG (158 kDa), ovalbumin (44 kDa), myoglobin (17 kDa), vitamin B12 (1.35 kDa).

3.4.2. CO-IMMUNOPRECIPITATION EXPERIMENTS

Protein A agarose resin (40 µl) was re-suspended in binding buffer [50 mM Tris/HCl (pH 7.5), 10 mM $MgCl_2$, 150 mM NaCl, 0.1% Triton] and conjugated with anti-hCdc45 antibodies. Samples (final volume of 50 µl) contained 0.4 µg of human Cdc45 or 7µg of each Mcm10 truncated form separately, or a combination of 0.4 µg of Cdc45 and 7µg of each Mcm10 truncated form. Protein A agarose resin conjugated with anti-Cdc45 antibodies (10 µl) was added to each sample. After incubation for 1 h at 4 °C with gentle shaking, the resin of each mixture was washed with 2 ml of binding buffer and then re-suspended in 30 µl of SDS/PAGE loading buffer 1x [50 mM Tris/HCl (pH 6.8), 10% glycerol, 200 mM β-mercaptoethanol, 0.5% SDS, 0.01% blue bromophenol]. Samples were run on a 10% SDS-polyacrylammide gel and transferred to a polyvinylidene difluoride membrane. The upper part of the membrane was analyzed with anti-hCdc45 rabbit polyclonal antibodies and anti-rabbit IgG antibodies conjugated with horseradish peroxidase using the ECL^+ system (GE Healthcare). The lower part of the

membrane was analyzed with anti-Histidine 6x tag rabbit polyclonal antibodies, anti-Mcm10-CTD rabbit polyclonal antibodies and anti-rabbit IgG antibodies conjugated with horseradish peroxidase using the ECL$^+$ system.

Co-immunoprecipitation on cell extracts were done using HEK293T ($0.6x10^6$ cells). HEK293T cell extract was prepared by washing cells in cold-ice PBS and lysed with 600 µl of IP buffer [20mM Hepes (pH 7.5), 150 mM KCl, 2mM EDTA, 1 mM DTT, 0.1% Triton, 1mM Na_3VO_4, 1mM NaF, 5% glycerol, protease and phosphatase inhibitors (Roche)]. Extract was first cleared of non-specific binders with the addition of 10 µl of protein A Agarose for 1 h at 4°C with gentle shaking. Separately, 10 µl of protein A Agarose was conjugated with anti-hCdc45 antibodies and 10 µl of the same resin was conjugated with pre-immune serum. Cleared extract was then combined with the resin conjugated with anti-hCdc45 antibodies or pre-immune serum (300 µl of extract for each) for 1 h at 4°C with gentle shaking. After the incubation the resin was washed with 2 ml of IP buffer and then re-suspended in 30 µl of SDS/PAGE loading buffer 1 x. Samples were run on a 10% SDS-polyacrylammide gel and transferred to a polyvinylidene difluoride membrane. The upper part of the membrane was analyzed with anti-hMCM10 rabbit polyclonal antibodies and detected anti-rabbit IgG antibodies conjugated with horseradish peroxidase using ECL system (GE Healthcare). The lower part of the membrane was analyzed using anti-hCdc45 rat monoclonal antibodies and detected with anti-rat IgG antibodies conjugated with horseradish peroxidase using ECL system (GE Healthcare).

3.4.3. SURFACE PLASMON RESONANCE MEASUREMENTS

Interaction of Cdc45 and Mcm-CTD were monitored by using the surface plasmon resonance biosensor system Biacore 2000 (Biacore, Uppsala, Sweden). Human Cdc45 [3000 resonance units (RU)] was coupled to the surface of a CM5 sensor chip in 10 mM sodium acetate buffer (pH 3.5), according to the manufacturer's instructions. To collect sensorgrams, the indicated protein was passed over the sensor surface at flow rate 10 µl/min at various concentrations. Recorded sensorgrams were normalized to a baseline of 0 RU and analyzed using the BIA Evalutation software (version 3.2).

3.4.4. DNA SUBSTRATES

The sequence of the synthetic oligonucleotides used to prepare the DNA substrates is reported in Table 1.

Oligonucleotides were labeled using T4 polynucleotides kinase and [γ-^{32}P]ATP. After the labeling reaction oligonucleotides were purified using a Micro Bio-Spin P-30 Tris chromatography column (Bio-Rad), according to the manufacturer's protocol. To prepare duplexes DNA molecules, mixtures were incubated for 5 min at 95 °C which contained the labeled and complementary unlabelled oligonucleotides at a 1:3 molar ratio. The samples were then slowly cooled at room temperature (25 °C).

3.4.5. DNA BAND-SHIFT ASSAYS

For each substrate, 10-µl mixtures were prepared which contained 50 fmol of [^{32}P]-labeled DNA in 20 mM Tris/HCl (pH 7.5), 3.5 mM β mercaptoethanol, 150mM NaCl, 10% glycerol and the indicated amounts of the different proteins. Following incubation for 15 min at room temperature, complexes were separated by electrophoresis through 5% polyacrylamide/bis gels (37.5:1) in 0.5 x TBE [100 mM Tris/HCl pH 8.3, 2 mM EDTA and 85 mM boric acid]. Radioactive signals (the shifted DNA against the free probed DNA for each lane) were quantified using a Storm PhosphorImager (Molecular Dynamics; Image Quant software) and subtracted of the blank. The values obtained were plotted against the amount of proteins used for each experiment. The kinetic parameters were calculated using Graph Pad Prism 3.0 Software.

3.4.5. DOMAIN STRUCTURE FITTING

3D EM map of Mcm10 and domain fitting illustrations were generated using PyMOL (http://pymol.org/). Surface rendering was performed using a threshold level of ~2 standard deviations (1σ) in the maps corresponding to 100% of the expected mass of the complex. The threshold was determined assuming protein density of 0.84 kDa/Å^3. For the docking, we used atomic coordinates of xenopus Mcm10 core domain (ID) [PDB: 3ebe], xenopus ID in complex with ssDNA [PDB: 3h15], and for the C-terminal Zn-binding domain [PDB: 2kwq]. Fitting of

atomic models was performed using Chimera (http://www.cgl.ucsf.edu/chimera).

References

3.5. REFERENCES

- Apger J, Reubens M, Henderson L, Gouge CA, Ilic N, Zhou HH, Christensen TW. (2010) Multiple functions for Drosophila Mcm10 suggested through analysis of two Mcm10 mutant alleles. *Genetics* **185,** 1151-65
- Bell SP, Dutta A. (2002) DNA replication in eukaryotic cells. *Annu Rev Biochem.* **71,** 333-74
- Bochkarev A, Bochkareva E. (2004) From RPA to BRCA2: lessons from single-stranded DNA binding by the OB-fold. *Curr Opin Struct Biol.* **14,** 36-42
- Chattopadhyay S, Bielinsky AK. (2007) Human Mcm10 regulates the catalytic subunit of DNA polymerase-alpha and prevents DNA damage during replication. *Mol Biol Cell.* **18,** 4085-95
- Eisenberg S, Korza G, Carson J, Liachko I, Tye BK. (2009) Novel DNA binding properties of the Mcm10 protein from Saccharomyces cerevisiae. *J Biol Chem.* **284,** 25412-20
- Fien K, Hurwitz J. (2006) Fission yeast Mcm10p contains primase activity. *J Biol Chem.* **281,** 22248-60
- Gregan J, Lindner K, Brimage L, Franklin R, Namdar M, Hart EA, Aves SJ, Kearsey SE (2003) Fission yeast Cdc23/Mcm10 functions after pre-replicative complex formation to promote Cdc45 chromatin binding. *Mol Biol Cell* **14,** 3876-87
- Hart EA, Bryant JA, Moore K, Aves SJ (2002) Fission yeast Cdc23 interactions with DNA replication initiation proteins. *Curr Genet.* 41, 342-8
- Heller RC, Kang S, Lam WM, Chen S, Chan CS, Bell SP. (2011) Eukaryotic origin-dependent DNA replication in vitro reveals sequential action of DDK and S-CDK kinases. *Cell* **146,** 80-91
- Hingorani MM, O'Donnell M. (1998) *Curr Biol.* **8,** R83-6. Review
- Izumi M, Yanagi K, Mizuno T, Yokoi M, Kawasaki Y, Moon KY, Hurwitz J, Yatagai F, Hanaoka F. (2000) The human homolog of Saccharomyces cerevisiae Mcm10 interacts with replication factors and dissociates from nuclease-resistant nuclear structures in G(2) phase. *Nucleic Acids Res.* **28,** 4769-77

- Kanke M, Kodama Y, Takahashi TS, Nakagawa T, Masukata H. (2012) Mcm10 plays an essential role in origin DNA unwinding after loading of the CMG components. *EMBO J.* **31,** 2182-94
- Krastanova I, Sannino V, Amenitsch H, Gileadi O, Pisani FM, Onesti S. (2012) Structural and functional insights into the DNA replication factor Cdc45 reveal an evolutionary relationship to the DHH family of phosphoesterases. *J Biol Chem.* **287,** 4121-8
- Lei M, Tye BK. (2001) Initiating DNA synthesis: from recruiting to activating the MCM complex. *J Cell Sci.* **114,** 1447-54
- Merchant AM, Kawasaki Y, Chen Y, Lei M, Tye BK. (1997) A lesion in the DNA replication initiation factor Mcm10 induces pausing of elongation forks through chromosomal replication origins in Saccharomyces cerevisiae. *Mol Cell Biol.* **17,** 3261-71
- Okorokov AL, Waugh A, Hodgkinson J, Murthy A, Hong HK, Leo E, Sherman MB, Stoeber K, Orlova EV, Williams GH. (2007) Hexameric ring structure of human MCM10 DNA replication factor. *EMBO Rep.* **8,** 925-30
- Patel SS, Picha KM (2000) Structure and function of hexameric helicases. *Annu Rev Biochem* **69,** 651–697
- Ricke RM, Bielinsky AK (2004) Mcm10 regulates the stability and chromatin association of DNA polymerase-alpha. *Mol Cell* **16,** 173-85
- Ricke RM, Bielinsky AK. (2006) A conserved Hsp10-like domain in Mcm10 is required to stabilize the catalytic subunit of DNA polymerase-alpha in budding yeast. *J Biol Chem*. **281,** 18414-25
- Robertson PD, Warren EM, Zhang H, Friedman DB, Lary JW, Cole JL, Tutter AV, Walter JC, Fanning E, Eichman BF. (2008) Domain architecture and biochemical characterization of vertebrate Mcm10. *J Biol Chem.* 283, 3338-48
- Robertson PD, Chagot B, Chazin WJ, Eichman BF. (2010) Solution NMR structure of the C-terminal DNA binding domain of Mcm10 reveals a conserved MCM motif. *J Biol Chem.* **285,** 22942-9
- Stauffer ME, Chazin WJ. (2004) Structural mechanisms of DNA replication, repair, and recombination.*J Biol Chem.* **279,** 30915-8 Review

- van Deursen F, Sengupta S, De Piccoli G, Sanchez-Diaz A, Labib K. (2012) Mcm10 associates with the loaded DNA helicase at replication origins and defines a novel step in its activation. *EMBO J.* **31**, 2195-206
- Warren, EM, Eichman, BF (2008) Structural basis for DNA binding by replication initiator mcm10. *Structure* **16,** 1892-1901
- Warren EM, Huang H, Fanning E, Chazin WJ, Eichman BF. (2009) Physical interactions between Mcm10, DNA, and DNA polymerase alpha. *J Biol Chem.* **284,** 24662-72
- Watase G, Takisawa H, Kanemaki MT. (2012) Mcm10 plays a role in functioning of the eukaryotic replicative DNA helicase, Cdc45-Mcm-GINS. *Curr Biol.* **22,** 343-9
- Wohlschlegel JA, Dhar SK, Prokhorova TA, Dutta A, Walter JC. (2002) Xenopus Mcm10 binds to origins of DNA replication after Mcm2-7 and stimulates origin binding of Cdc45. *Mol. Cell* **9,** 233-40
- Xu X, Rochette PJ, Feyissa EA, Su TV, Liu Y. (2009) MCM10 mediates RECQ4 association with MCM2-7 helicase complex during DNA replication. *EMBO J.* 28, 3005-14
- Zhu W, Ukomadu C, Jha S, Senga T, Dhar SK, Wohlschlegel JA, Nutt LK, Kornbluth S, Dutta A. (2007) Mcm10 and And-1/CTF4 recruit DNA polymerase alpha to chromatin for initiation of DNA replication. *Genes Dev.* **21,** 2288-99